TECHNICAL REPORT ECOM-00240-F, VOL. I

MONTE CARLO CODES FOR STUDY OF LIGHT TRANSPORT IN THE ATMOSPHERE

Volume I: Description of Codes

FINAL REPORT

By

D. G. COLLINS - M. B. WELLS

AUGUST 1965

ECOM

UNITED STATES ARMY ELECTRONICS COMMAND • FORT MONMOUTH, N.J.

CONTRACT DA28-043 AMC-00240(E)

RADIATION RESEARCH ASSOCIATES, INC.

Fort Worth, Texas

TECHNICAL REPORT ECOM-00240-F, VOL. I AUGUST 1965

MONTE CARLO CODES FOR STUDY OF LIGHT TRANSPORT IN THE ATMOSPHERE

Volume I: Description of Codes

FINAL REPORT

1 JULY 1964 TO 31 JULY 1965

CONTRACT NO. DA 28-043 AMC-00240(E)

DA PROJECT NO. IVO 14501-B-53A-13-03

DASA SUBTASK NO. DASA 1304-01/12.017

Prepared by

D. G. COLLINS AND M. B. WELLS

RADIATION RESEARCH ASSOCIATES, INC.

FORT WORTH, TEXAS

For

U. S. ARMY ELECTRONICS COMMAND, FORT MONMOUTH, N. J.

ABSTRACT

Monte Carlo procedures designated as LITE-I and LITE-II were developed to study the transport of light through the earth's atmosphere under various environmental conditions. LITE-I treats monochromatic light emitted from a point source, and LITE-II treats monochromatic plane sources of light. The codes have been written in both ALGOL for the Burroughs B-5000 and FORTRAN II for other computers. The codes are sufficiently flexible to treat multiple scattering in an atmosphere in which air density and aerosol size distribution vary independently and arbitrarily with altitude. Provision for treating ground and cloud reflection with an albedo method is also available in the codes.

The codes have been verified through comparisons with other calculations of light transport in the atmosphere. Utilization instructions, input data formats, sample problems, and the ALGOL listings of the codes are given to aid those who wish to utilize the codes.

FOREWORD

The authors wish to express their appreciation to Henrietta Hendrickson and Hemma Francis of Oak Ridge National Laboratory who aided in the checkout and running of test problems on the FORTRAN versions of the LITE codes. They also wish to acknowledge the assistance of Leon Leskowitz, of the U. S. Army Electronics Laboratory, Fort Monmouth, New Jersey, for his assistance in translating the FORTRAN codes to the ALGOL language and his many helpful suggestions during the checkout of the ALGOL versions of the LITE codes. The work described in this report was carried out under the technical monitorship of Dr. R. W. Fenn of the Atmospheric Science Laboratory, USAECOM, Fort Monmouth, New Jersey.

TABLE OF CONTENTS

LIST OF FIGURES

LIST OF TABLES

I. INTRODUCTION

In order to predict the degree of thermal radiation damage that may occur from nuclear detonations, the effects of various atmospheric and terrain conditions upon the propagation of light energy must be evaluated. During recent years, considerable emphasis has been placed on both theoretical and experimental aspects of light transport in the atmosphere. Typical of the experimental data are observations reported by Canter and Petriw (Reference 1). They measured the scattered light intensities from a point source above partially and totally snow-covered terrain in which the surface albedo varied from approximately 0.2 to about 1.0. Some of their observations were made during cloud cover, providing data on the "duct effect" or energy trapping situations. Curcio, Kenestrick and Cosden (References 2, 3, 4 and 5) made a thorough study of light scattered by the atmospheric aerosol. Many of their observations were conducted over the water surface using a collimated source and receiver arrangement that reduced the detection of any surface reflected light.

The U. S. Naval Radiological Defense Laboratory has also conducted experimental studies (References 6, 7, 8 and 9) on the transmission of light emitted by a 4π source through the atmosphere. The results of their measurements give information on the scattered-to-direct intensity as a function of both source-receiver range and receiver angle for the source and receiver located near the air-ground interface. The USNRDL measurements give data on the scattering of light in the atmosphere for atmospheric conditions ranging from very clear (visibility 15+ miles) and for various conditions of cloud cover.

In general, these experimental data indicate that the transport of light within the earth's atmosphere is highly dependent upon both the meteorological and terrain conditions. This dependence is so great that it is difficult to apply measurements made at one time and place to predict the scattered light intensity at some other time or place. Experimental investigations of the intensity of light at a given receiver point as a function of a single parameter, such as the surface albedo, are hampered by the inability of the investigator to control all of the other environmental parameters.

Several of the experimental data for point sources in the atmosphere have been used to derive semi-empirical relations which will allow prediction of the light intensity as a function of distance from an uncollimated source. Typical of these semi-empirical relations are those derived by Stewart-Curio (Reference 12), and Gibbons (Reference 8). All of these semi-empirical relations correlate the uncollimated transmission with the extinction coefficient and the path length. To account for ground albedo or cloud-cover reflections, some correction factor is usually applied to these relations. At the present time, there is no general agreement on the magnitude of the correction due to ground and cloud albedo and the dependence of the correction factor on the source-receiver distance, or the wave length of the source radiation. It should also be noted that there is considerable disagreement between the results obtained from these semi-empirical relations at distances larger than a few kilometers.

Much of the theoretical work published on light scattering has obvious limitation for, in many cases, the calculational methods

developed are beset with difficulties when extensions are made to other than simple models. The Boltzman transport equation, which rigorously defines the transport of light, is generally written in intractable form, and many fidelity-reducing procedures have been applied to the transport equation in order to obtain solutions. These include replacing an inhomogeneous medium with a homogeneous medium, the use of isotropic scattering, instead of the highly anisotropic scattering usually found in nature, or the dismissal of scattering orders greater than the first as negligible.

Coulson, Dave and Sekera (Reference 10) published a rather complete set of calculated data on the transmission and reflection of a broad beam of light incident on the top of a planetary atmosphere with Rayleigh scattering. Their method of calculation was that derived by S. Chandrasekhar (Reference 11). Although the calculational method is rigorous for the model considered, it is not applicable to atmospheres involving scattering processes other than Rayleigh scattering, or point sources of light.

It appears that there is a need for a calculational method which does not require the use of fidelity-reducing procedures and which would provide a means of studying the effects of parameters such as cloud cover, ground albedo, and atmospheric aerosol content on the transport of light in a controlled atmosphere. Such a calculational method should also be capable of studying the transport in air of light emitted by both point and broad beam sources. One method that has the capability of satisfying all of the above requirements is the Monte Carlo method.

The Monte Carlo method is distinguished by its experimental nature. It involves the use of statistical sampling techniques to approximate the solution of a mathematical or physical problem. The application of the Monte Carlo method to the problem of light transport in the atmosphere makes use of the fact that the radiation transport equation can be reduced to a probabilistic model of particle behaviour. The solution of the transport equation can then be realized by averaging the results of individual particle histories, where the history of each individual particle exhibits a random behaviour in accordance with the probabilistic model.

A preliminary study on the application of Monte Carlo methods to the light transport problem was performed using Monte Carlo codes that had originally been developed for the study of neutron transport. The results of this preliminary study are described in Section II of this report.

As the result of the preliminary study on the application of Monte Carlo methods to light transport problems, it became apparent that the Monte Carlo method could provide a means of treating rigorously the multiple scattering of light by both molecules and aerosol particles in a slab geometry atmosphere. Two machine programs were developed which have been designated as LITE-I and LITE-II. LITE-I allows for treatment of problems involving point sources and LITE-II treats problems involving broad beam sources. The LITE codes were originally written in FORTRAN-II language for the IBM-7090 computer. Following checkout and debugging of the FORTRAN codes, they were converted to ALGOL language codes by the use of a FORTRAN-to-ALGOL

Translator for the Burroughs B-5000 computer. In Section III, a detailed presentation of the methods utilized in the LITE codes is given. Section IV shows comparisons of LITE codes results with several other sets of calculated data.

A listing of the ALGOL language codes and the utilization instructions for the codes are presented in Volume II of this report. Also presented in Volume II are listings of a sample problem input and output for each of the LITE codes.

II. PRELIMINARY INVESTIGATIONS

The objective of the preliminary investigations was to show that the transport equation describing light transport in the atmosphere is amendable to solution by Monte Carlo techniques through the use of existing Monte Carlo codes which were developed for the purpose of studying neutron and gamma-ray transport. The results of the Monte Carlo calculations obtained from the use of the nuclear radiation transport codes were to provide information on the important parameters to be considered in the formulation of a Monte Carlo code which was to be developed for the purpose of studying light transport in an air-ground geometry.

An initial study was conducted to investigate the effect of higher order scattering on the total scattered intensity for a point source and receiver located in an air-ground geometry. The study was conducted using the L05 Monte Carlo code (Reference 13) which allowed a description of an air-ground geometry by considering the ground as a dense layer of atmosphere in which scattering was assumed isotropic in the laboratory system.

The change in atmospheric density was approximated with ten slab layers of atmosphere with decreasing densities. The extinction cross section for air at ground level was taken to be 4.403×10^{-6} cm^{-1}. The Rayleigh and Mie scattering cross sections were taken to be 2.523×10^{-6} cm^{-1} and 1.88×10^{-6} cm^{-1} respectively. The phase function for Mie scattering was taken to be that computed for an aerosol particle size distribution proportional to r^{-3}, where r is the particle radius. The extinction, Rayleigh scattering, and Mie scattering

cross sections were allowed to vary in the same manner as the atmospheric density varys with altitude. The L05 code was used to compute the scattered light intensity from a point isotropic light source located 1 km above the ground surface for a point receiver located at ground level 10 km horizontal dist nce from the source (a source-receiver separation distance of 4.4 mean-free-path lengths). A ground albedo of 0.5 was approximated in the calculations by selecting the proper scattering-to-total cross section ratio for the ground layer. The scattering-to-total cross section ratio used in the L05 calculations for the ground layer was obtained from calculations reported by Rafalski (Reference 14) which gives the neutron albedo as a function of the scattering-to-total cross section ratio for a medium in which scattering is isotropic in the laboratory system and in which no energy degradation is allowed. A plot of Rafalski's calculations of the albedo versus the scattering-to-total cross section ratio is shown in Figure 1. Figure 2 shows the results obtained from five L05 problems in which the maximum number of collisions allowed per history was taken as 5, 10, 20, 30 and 40, respectively. The results obtained from problems with sample sizes of 1000 histories show that the scattered intensity at the receiver position increases with an increase in the maximum number of collisions allowed per history up through a maximum of approximately 20 collisions per history. The scattered intensities for problems involving more than 20 collisions per history are approximately equal. The calculated point shown in Figure 2 for a maximum of 20 collisions per history has a large standard deviation and is felt to be too high, particularly since the scattered intensities for 30 and 40 maximum collisions per history are both below the value computed for 20 collisions.

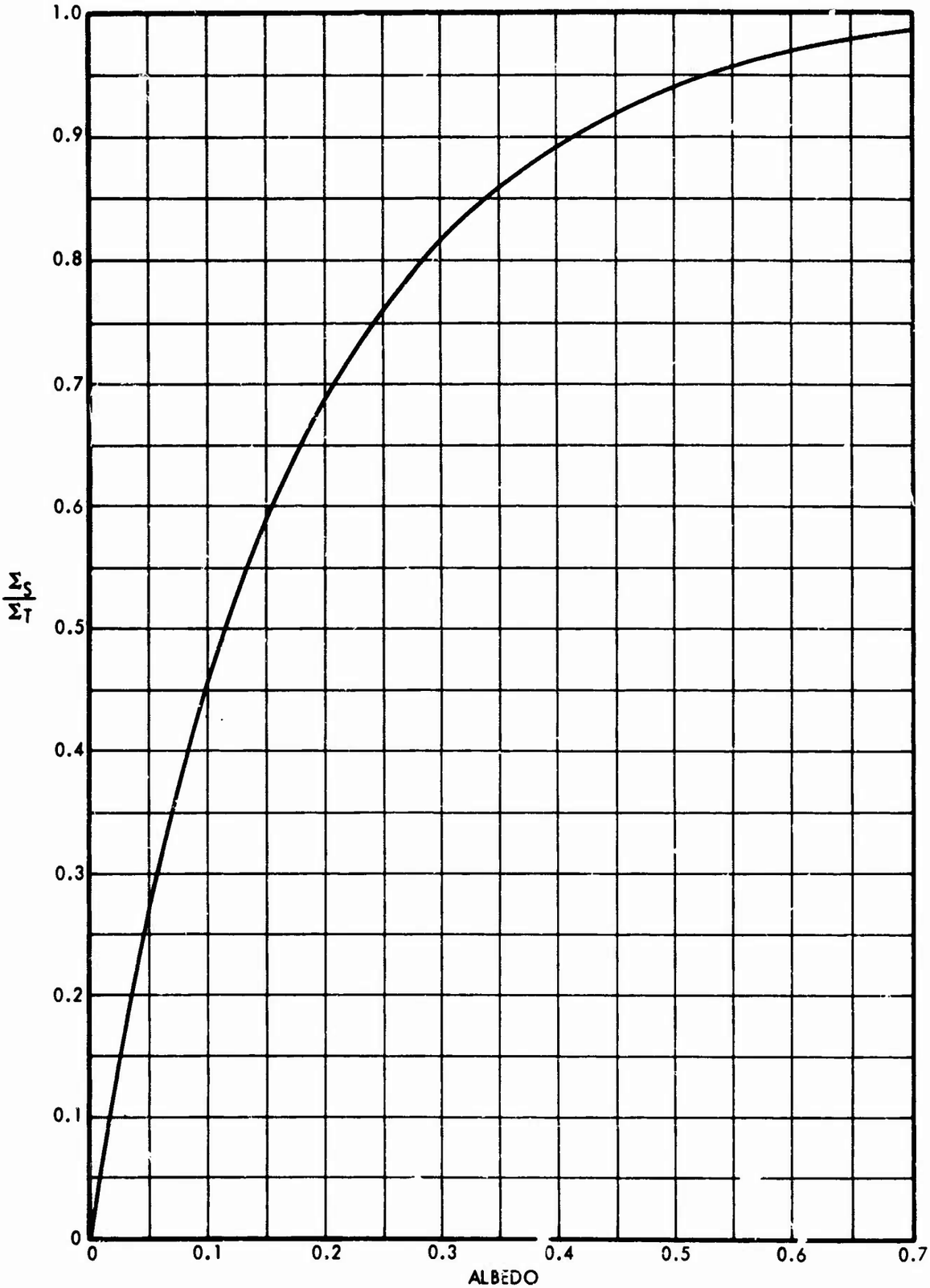

Fig. 1. Dependence of the Scattering-to-Total Cross Section Ratio on the Albedo

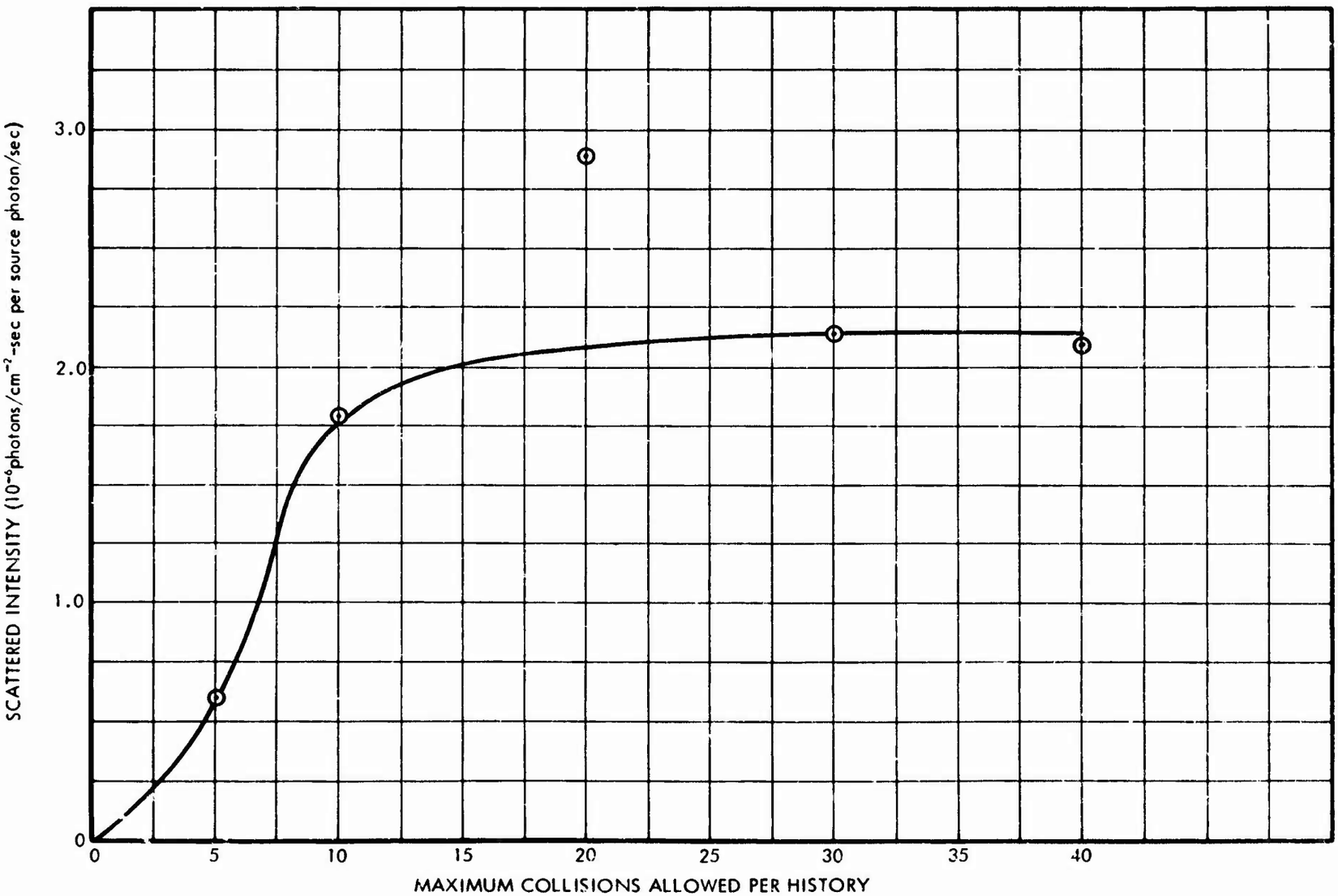

Fig. 2. Dependance of the Scottered Flux at 4.4 Meon-Free-Poths from o Point Isotropic Light Source on the Maximum Number of Collisions Allowed per History

Some additional information on the five L05 problems is given in Table I. It is noted that although the average number of collisions per history increases as the maximum number allowed increases, the average number of collisions per history appears to be reaching a maximum value as the number of maximum collisions allowed per history increases to 40. The fact that a maximum value in the average number of collisions followed per history will be reached is indicated by the increase in the number of histories terminated by particle escape from the problem geometry (leakage into the atmosphere above 30 km). From the results shown in Figure 2 and Table I, it appears that valid results for scattered intensities can be obtained from L05 calculations in which the maximum number of collisions allowed per history is 20, provided that an adequate number of histories are treated.

Since the maximum number of collisions that should be considered in any given problem is a function of the geometry of the particular problem, it was decided that the light transport code to be developed should provide information on the scattered intensity resulting from each order of scattering. This will allow an inspection of the results to determine whether the intensity for the highest order of collision allowed adds significantly to the total scattered intensity.

In order to determine the geometric effects of an air-ground geometry on the transport of light, two additional L05 problems were run for a point isotropic light source where the source-receiver separation distances were 1.5 and 3 mean-free-path lengths respectively. The results of the three L05 problems were then compared with the

Table I. Dependence of Various Parameters on Maximum Number of Collisions Allowed Per History in L05 Problems

Maximum No. of Collisions Allowed per History	Fraction of Histories Terminated by Geometry	Fraction of Histories Terminated by Max. Coll.	Average No. of Collisions per History	Intensity of Scattered Light
5	0.474	0.526	3.239	6.028-7 *
10	0.623	0.377	5.649	1.785-6
20	0.707	0.293	9.312	2.891-6
30	0.769	0.231	11.788	2.130-6
40	0.822	0.178	12.968	2.094-6

* Read 6.028-7 as 6.028×10^{-7}

total intensities calculated for the respective source-receiver separation distances for the source and receiver embedded within an infinite media. The infinite media data were obtained using the K74 Monte Carlo code (Reference 15) and the properties of the infinite media were identical to those of the lower layer of the atmosphere in the L05 problems. Figure 3 shows a comparison of the L05 and the K74 data. The intensities shown have been multiplied by $4\pi R^2$, where R is the slant range between the source and receiver. The differences between the K74 and the L05 results should be a measure of the effect of a varying atmospheric density and of the air-ground interface on light transport in air. The direct intensity times $4\pi R^2$ is also shown in Figure 3 and was determined to be the same with both codes. The differences between the K74 and L05 total intensity curves and the direct intensity curve are the scattered intensities received by an isotropic receiver.

Since the geometric effects of an air-ground geometry greatly affect the scattered light intensity, it was decided that the light transport code to be developed should print the scattered intensity in a form that would allow the geometric effects to be analyzed. In particular, the scattered intensities should be printed as a function of both the region of scatter and the number of times a particle has reflected from a given reflection surface.

The importance of multiple scattering was also investigated for a broad beam source of light incident upon an infinite plane-parallel Rayleigh atmosphere of 5 mean-free-paths in thickness. This study was conducted using the C-18 Monte Carlo slab penetration code

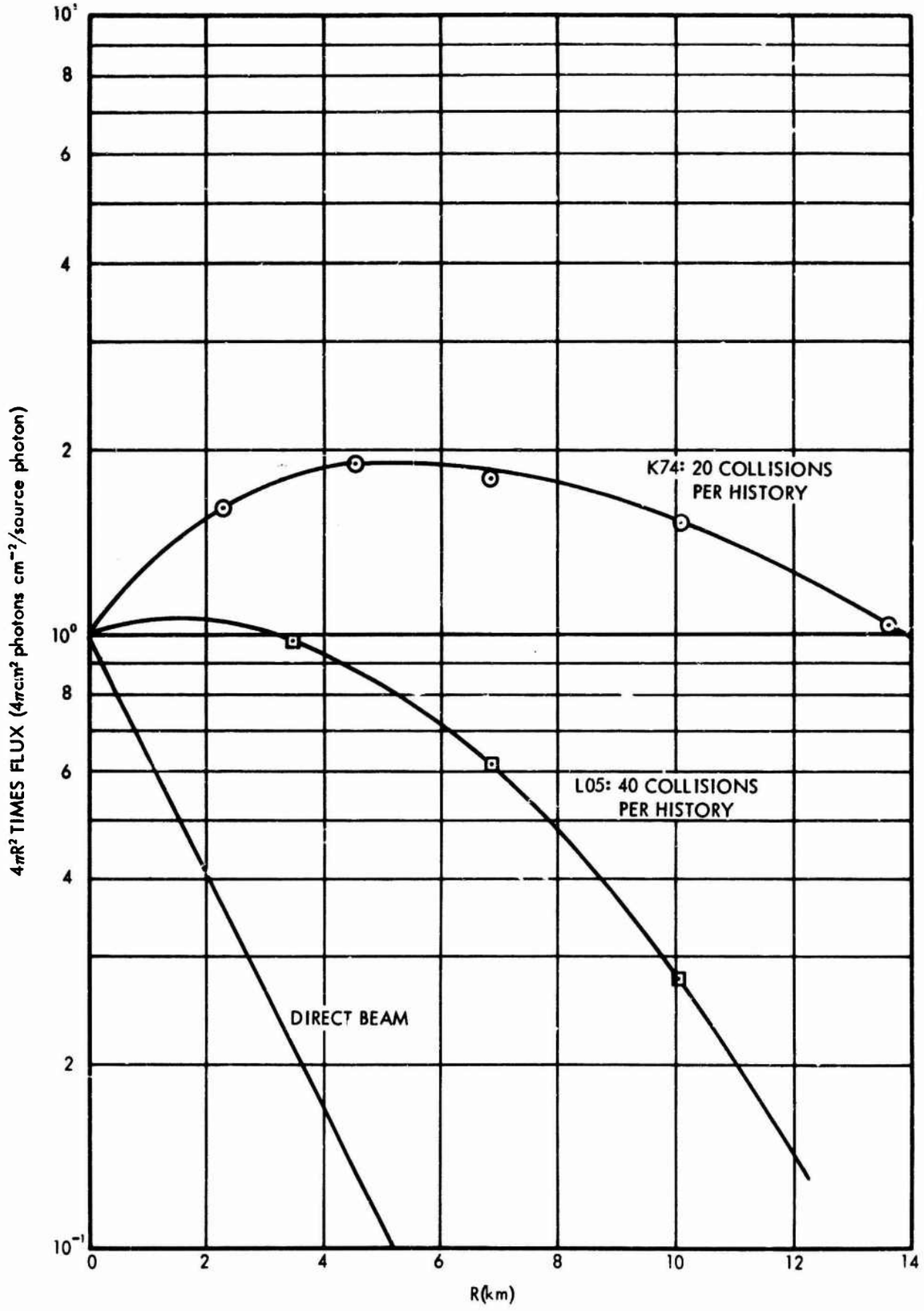

Fig. 3. Comparison of Calculations of Photon Flux Times Distance Squared for Infinite Medium and Air-Ground Geometries

(Reference 16). Light from a broad beam source was taken to be incident normal to the atmosphere, and the total intensity was calculated at various depths in the slab. Figure 4 presents the results obtained for the total intensity after a given number of collisions as a function of depth into the atmosphere. The importance of multiple scattering is seen to increase as a function of depth into the atmosphere. The intensity after 30 collisions is only a factor of 1.6 greater than the intensity after 5 collisions for a depth of 1 mean-free-path, whereas the intensity after 30 collisions is a factor of 4 greater than that after 5 collisions for a depth of 5 mean-free-paths.

A set of three LO5 problems were run to compare with light scattering data supplied by USAEL which were taken during an Everglades, Florida experiment. Although detailed information concerning the ground albedos for this data were not available, the albedos were estimated in order that a rough comparison might be made. The three LO5 problems were designed to calculate the scattered and direct intensities received by a flat plate receiver at distances of 1, 2, 3, 5 and 7 miles for both blue and green light. The light source was located 70 feet above ground level and the receiver points were located 12 feet above the ground. The extinction coefficients used for each wave length, as well as the phase functions, were obtained from the measured data. The scattering-to-total cross section ratio of the ground media was selected to simulate a ground albedo of approximately 0.5. The results for the green light source are presented in Figure 5, where they are compared with measured data. Since the source intensity was not given, the magnitude of the measured intensities were

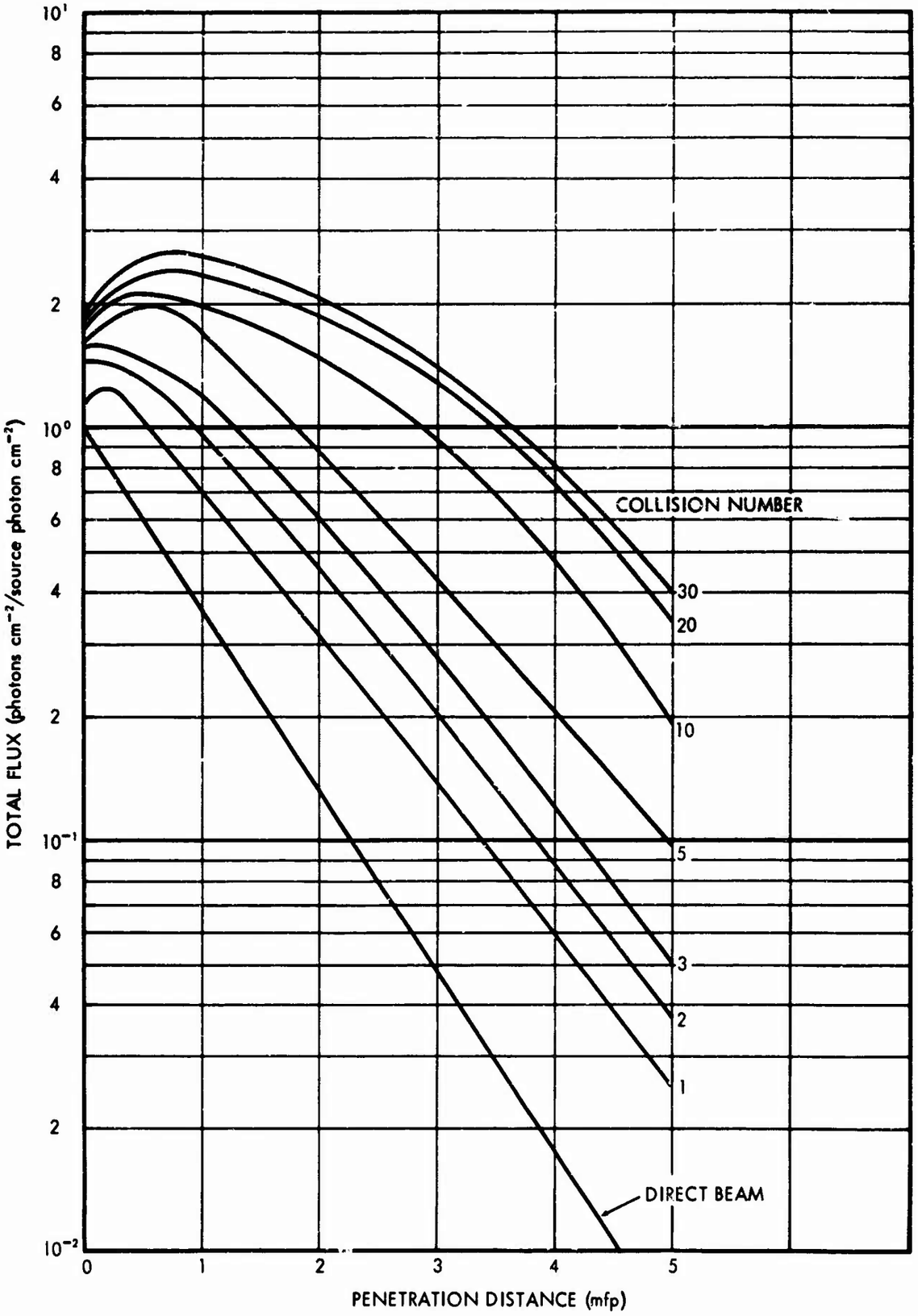

Fig. 4. Variation of the Total Flux After a Given Number of Collisions with Penetration Distance

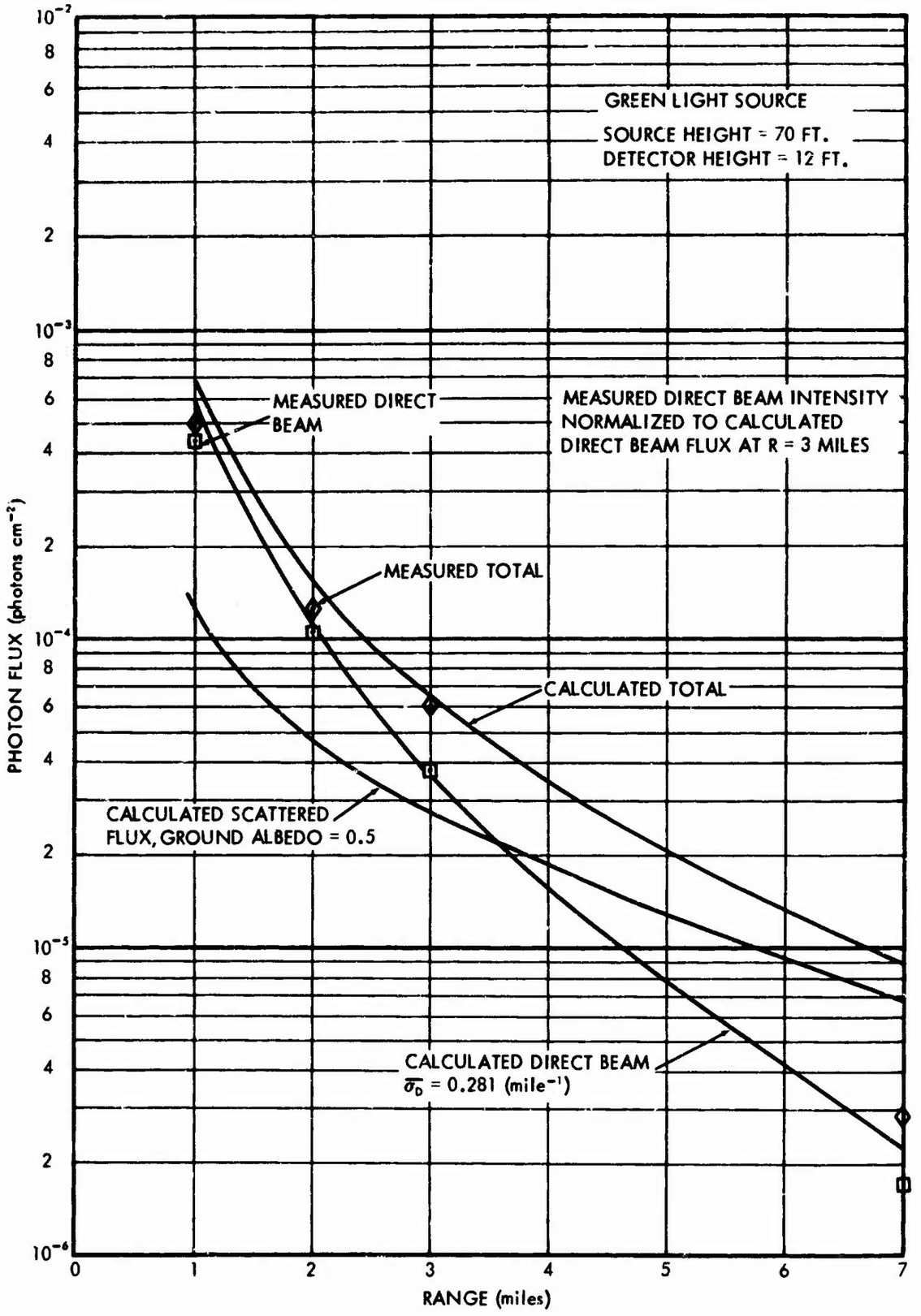

Fig. 5. Light Intensity Received by a Flat Plate Receiver as a Function of Slant Range: Ground Albedo = 0.5

normalized to the calculated direct intensity at the 3 mile distance. The agreement between the measured and calculated data are rather good, except for the point at seven miles where the calculated data greatly overpredicts the measured intensities. It is thought that the ground albedo of 0.5 is probably too high for the Everglades terrain. A high albedo would have a greater effect on the 7 mile point than on the other points. Figure 6 shows a comparison of the calculated and measured data for blue light. The results of an additional calculation for a ground albedo of zero are also shown in Figure 6. It is seen that the data for the zero ground albedo agree better with the measured intensities than do the results for the 0.5 ground albedo. The overall agreement between the two sets of measured and calculated data lends confidence in the use of Monte Carlo methods to predict scattered intensity of light in an air-ground geometry.

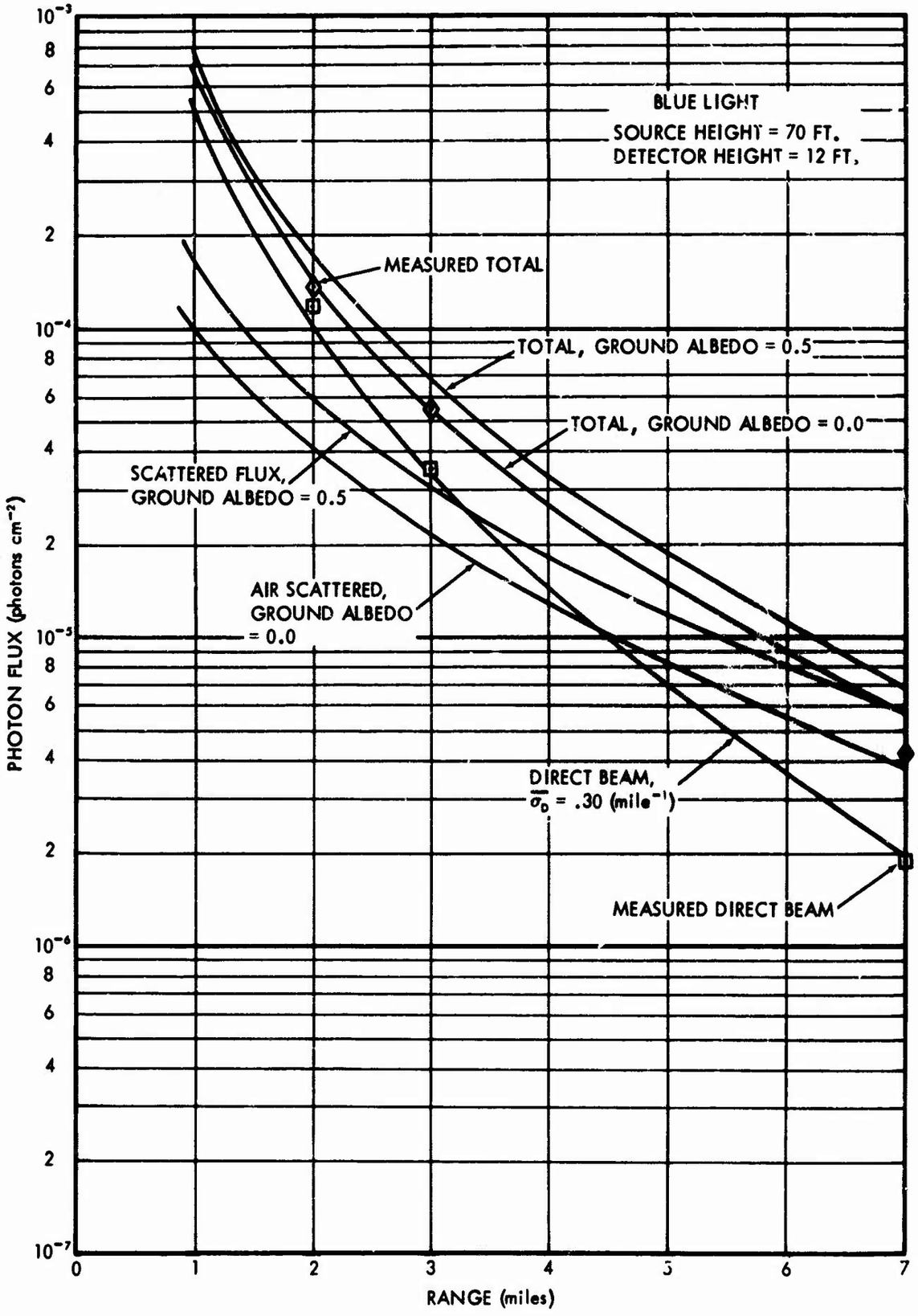

Fig. 6. Comparison of Calculations of Light Transport in Which the Ground Albedo was Taken to be 0.5 and 0.0

III. METHODS

The favorable results obtained with the nuclear radiation shielding codes L05, K74 and C18 during the preliminary investigations of light transport in the atmosphere led to the development of two Monte Carlo procedures designed specifically for the study of light transport. The first of these procedures was developed for use in studying the transport of light emitted isotropically or with an arbitrary polar angular distribution by a point source located in an air-ground geometry. This procedure has been designated as the LITE-I code. The second procedure (LITE-II) was developed to study the transport of light emitted from a plane source with an arbitrary angular distribution located either at the top of an air-ground atmosphere or within the atmosphere.

The codes treat multiple scattering of monochromatic light in an atmosphere that may vary arbitrarily with altitude. Routines are available for treating both Rayleigh and Mie scattering events. An intermixture of the two events is possible or an atmosphere may be considered as either a Rayleigh or a Mie atmosphere. The Mie scattering phase functions are read as input for any given problem so the aerosol concentrations may be varied from one problem to another. The LITE codes do not consider polarization of light.

Albedo techniques are incorporated to treat both ground and cloud reflection; however, either the ground or cloud regions may be treated as regions of increased density rather than with the albedo method, if desirable.

Basically, the Monte Carlo codes treat light on a particle basis such that the weight assigned to each individual light particle represents either groups of photons or a fractional part of a photon. The path that an individual particle traverses in an air-ground medium is generated by a random selection of the particle's directions and distances between collisions. The initial direction is chosen from the input source angular distribution and the change in direction at each collision is determined by sampling a scattering angle from either the Rayleigh or Mie distribution depending upon which scattering process the particle has undergone. Distances between collisions are chosen by selecting a path length from either an exponential or a truncated exponential distribution and calculating the distance corresponding to that path length. A weight parameter initialized to a value of one is assigned to each source particle. Each time sampling from a biased distribution is conducted, the weight parameter is adjusted to remove the bias introduced.

At each collision an estimate, based upon the particle's weight, of the light intensity that would scatter directly to each of a set of one to ten receiver positions is made. Point omnidirectional receivers are used in the LITE-I code and plane receivers are used in the LITE-II code. One history, composed of the tracing of an individual particle through all orders of scattering until it is terminated, provides an estimate of the total scattered light intensity at each of the receiver positions. A final estimate of the scattered intensities is obtained by averaging the results for each of the individual histories.

In order to examine the statistical fluctuation of the results, the total number of histories may be subdivided into groups, each containing an equal number of histories such that any one group does not contain data for more than 500 histories. The average intensities for each individual group of histories are printed as a function of the order of collision and detector numbers. A visual examination of the statistical fluctuation is then possible by plotting the results for each of the groups.

Upon completion of the last group of histories the intensities at each receiver as a function of order of collision are averaged over the total number of groups and then printed. The deviation of the group results about this average is also calculated and printed. The scattered intensities at each receiver position are then printed as a function of angle and order of reflection for a given reflection surface. The scattered intensities are also printed as a function of region of scatter to aid in the determination of those regions which contribute most significantly to the scattered intensity.

In order to examine the amount of light reflected from all of the reflection surfaces to each receiver position, the reflected light intensities for each receiver are also printed. After the total scattered intensities are calculated and printed, the direct intensity at each receiver position is calculated and printed.

The following portions of Section III describe in detail the methods utilized in the LITE codes. The formulae presented are a mixture of the usual mathematical notation and that used in FORTRAN language. The * is used to denote multiplication and parentheses

are often used to enclose subscripts. The LITE-I code is discussed initially with a following discussion of those features in the LITE-II code that differ from the LITE-I code.

3.1 Description of LITE-I Code

3.1.1. Selection of Source Angles

The LITE-I code provides for the description of a point isotropic or point anisotropic source. The source is located on the vertical axis at a height HS above the air-ground interface. The angular distribution of the source is defined in terms of the cosine of the polar angle measured from the vertical H axis. It is assumed that the angular distribution is azimuthally symmetric. The input values PAG(J) defining the polar angular distribution are given by the expression

$$PAG(J) = \frac{\int_{CANG(1)}^{CANG(J)} -n(\cos\theta)d\cos\theta}{\int_{CANG(1)}^{CANG(NAG)} -n(\cos\theta)d\cos\theta} ,$$

where $n(\cos\theta)$ is the function describing the desired angular distribution,

CANG(J) are the input cosine values used in defining the angular distribution,

NAG is the number of input cosine values, and

PAG(1) = 0 for J = 1.

If the distribution is isotropic, $n(\cos\theta) = 1$ and

$$PAG(J) = \frac{1}{2}\,(CANG(1) - CANG(J)).$$

Selection of Cosine of Source Polar Angle

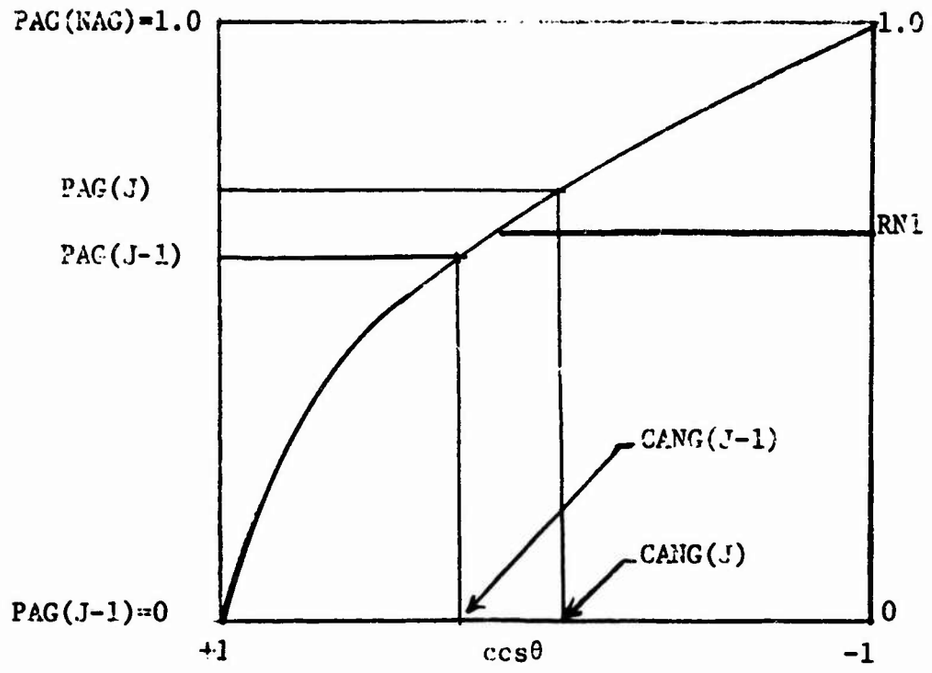

PAG(J) - PAG(J-1) is the probability of the particle being emitted within the interval from CANG(J-1) to CANG(J). The interval through which a particle is emitted is selected at random by locating the two values of PAG(J) such that PAG(J-1) $\leq$ RN1 $<$ PAG(J), where RN1 is a random number. The cosine of the emission angle is obtained by a linear interpolation with a second random number between the two values of CANG(J) that bound the interval

$$SANG = CANG(J-1) - RN2\,\left(CANG(J-1)-CANG(J)\right)$$

where SANG is the cosine of the source angle selected,

RN2 is a second random number, and

CANG(J) are the input cosines bounding the interval selected with the first random number.

For some problems it may be desirable to bias the sampling from the source polar angular distribution to improve the sampling in those directions which point toward the detector positions. The biased distribution is input into the code and the weight of the light particle is adjusted for its not having been sampled from the true angular distribution. If the true angular distribution is isotropic (NAOP = 0), then the code adjusts the particle weight internally with the expression

$$\text{WEIGHT(I)} = \left(\frac{1.0}{\text{PAG(I)} - \text{PAG(I-1)}}\right)\left(\frac{\text{CANG(I-1)} - \text{CANG(I)}}{\text{CANG(1)} - \text{CANG(NAG)}}\right) .$$

If the true distribution is anisotropic and a biased distribution is input (NAOP = 1), the weight adjustment factors WAG(J) must also be input. WAG(I) is the weight that is assigned to all particles emitted from the source with the cosines of their angles between CANG(I-1) and CANG(I). WAG(1) is not used by the code since PAG(1) is equal to 0 and the code never selects an I = 1. WAG(2) is the weight that will be assigned to particles emitted from the source with a cosine between CANG(1) and CANG(2). The WAG(J) values should be computed with the following equation,

$$\text{WAG(J)} = \frac{\int_{\text{CANG(J-1)}}^{\text{CANG(J)}} -n'(\cos\theta)d\cos\theta}{\int_{\text{CANG(J-1)}}^{\text{CANG(J)}} -n(\cos\theta)d\cos\theta}$$

where $n'(\cos\theta)$ is the true angular distribution, and

$n(\cos\theta)$ is the input biased distribution.

The LITE-I code presently treats only those source angular distributions that are azimuthally symmetric. Rather than selecting the azimuthal angle from an isotropic distribution, all source angles are

started with an azimuthal angle of 0°. Each time an estimate of the scattered intensity at a receiver is made, the azimuthal position of the receivers are selected from a uniform distribution between 0 and 2π. This produces the same results as selecting a source azimuthal angle from an isotropic distribution and estimating the light intensity at a receiver whose azimuthal position is fixed. The efficiency of the LITE-I code may be increased by selecting two or more azimuthal positions for a receiver point and averaging the contributions to all the positions from each collision. The process of selecting N receiver azimuthal positions and averaging the contributions to each position is equivalent to increasing the original number of histories by a factor of N. This process, however, results in a considerable amount of machine time saved since the same set of collision points is used N times.

3.1.2 Optical Path Lengths

Since the extinction coefficient for a clear atmosphere has been shown to differ considerably from the exponential variation at the upper end of the visible range and also below the visible range (Ref. 17), a method was developed to allow an arbitrary variation of extinction coefficient with altitude. Rather than inputting the extinction coefficient, the optical thickness from ground level to altitude hl,

$$\tau(hl) = \int_0^{hl} \Sigma(h)dh,$$

is input for values of hl sufficiently close enough together so as to adequately represent the curve $\tau(h)$ with straight line segments joining the $\tau(hl)$ values. $\Sigma(h)$ is the extinction coefficient at altitude h.

For a light particle located at an altitude hl and traveling in a direction making an angle θ with the vertical vector, the number of path lengths, RHO, traversed before collision is sampled from an exponential distribution if the particle's direction is downward or from a truncated exponential distribution if the particle's direction is upward. Sampling from the exponential distribution is accomplished by solving the integral equation

$$RN = \int_0^{RHO} e^{-\rho} d\rho \ ,$$

for RHO, when RN is a random number between 0 and 1. For the truncated exponential distribution the path length, RHO, is given by the equation,

$$RN = \int_0^{RHO} \frac{e^{-\rho} d\rho}{1-e^{-\rho_{max}}} \qquad 3.1.2.1$$

where ρ_{max} is the number of path lengths from the collision point at hl to the upper surface of the atmosphere along the particle's directional vector. The quantity ρ_{max} is given by the expression

$$\rho_{max} = \left(\tau(h_{max}) - \tau(hl)\right) / \cos\theta \qquad 3.1.2.2$$

where $\tau(h_{max})$ is the thickness of the atmosphere in mean-free-path lengths,

$\tau(hl)$ is the number of mean-free-path lengths from the ground to altitude hl, and

$\cos\theta$ is the cosine of the angle that the particle's directional vector makes with the positive vertical vector.

The solution of equation 3.1.2.2 for RHO gives

$$RHO = -\ln\left(1.0 - RN(1.0-e^{-\rho max})\right)$$

which reduces for $\rho_{max} = \infty$ to

$$RHO = -\ln(1.0 - RN) ,$$

the solution of equation 3.1.2.1, the case when the particle's direction is downward.

Sampling path lengths from the truncated exponential distribution introduces biasing since a collision is forced before the particle escapes the upper atmosphere. This biasing is removed by multiplying the particle's weight by

$$1 - e^{-\rho max},$$

the probability a collision will occur before it escapes the atmosphere.

Distance Between Collision

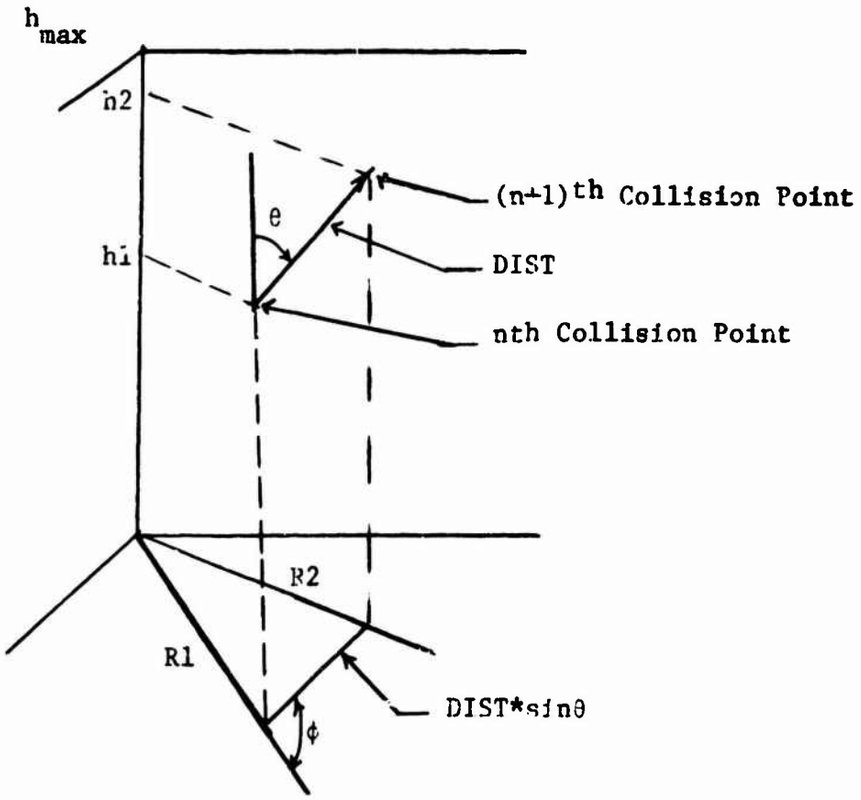

After the path length RHO has been sampled, the altitude of the next collision is determined by solving the expression

$$\tau(h2) = \tau(h1) + RHO*\cos\theta$$

and interpolating between the values of h1 corresponding to the two values of $\tau(h1)$ that bound $\tau(h2)$ to find the height h2 that corresponds to $\tau(h2)$.

The distance between collisions is computed with the formula

$$DIST = (h2 - h1)/\cos\theta$$

where h1 is the altitude of nth collision,

h2 is the altitude of the $(n+1)^{th}$ collision, and

$\cos\theta$ is the cosine of the angle between the line joining the two collision points and the positive vertical vector.

The radial position of the (n+1)th collision point is computed with the expression

$$R2 = \sqrt{R1^2 + (DIST*\sin\theta)^2 + 2*R1*DIST*\sin\theta*\cos\phi}$$

where R1 is the radial position of the nth collision,

$DIST*\sin\theta$ is the projection of the line joining the nth and (n+1)th collisions into the horizontal plane, and

$\cos\phi$ is the angle that the horizontal projection makes with a radial vector through the nth collision point.

3.1.3 Atmosphere Description

Since the aerosol size distribution and the variation of aerosol concentration with altitude may vary independently with air density, the ratios of the Rayleigh-to-scattering cross section and the ratios of the scattering-to-total cross section are input for the points h1

used in defining $\tau(h)$. The probability of Mie scattering at any altitude is then given by

$$1 - RAYR(h)$$

where RAYR(h) is the ratio of the Rayleigh-to-scattering cross section.

The variation of aerosol particle size distribution with altitude is treated by dividing the atmosphere into regions and defining a different Mie scattering phase function for each region. The Mie scattering angle for each Mie scattering event is chosen from the phase function for the region containing the collision point.

Light scattering within cloud layers can be considered by the code, if desired. If a cloud layer is located between heights HC1 and HC2, where HC1 and HC2 are the heights of the top and bottom of the cloud layer, then the extinction coefficient $\Sigma(h)$ used in the equation

$$\tau(h1) = \int_0^{h1} \Sigma(h)dh$$

for $HC1 \geq h \geq HC2$ should be that for the cloud layer. The values of the ratio RAYR(h) input for $HC1 \geq h \geq HC2$ should be the ratio of the Rayleigh to the total scattering cross section for the cloud layer. The cloud layer can be defined by one or more regions and different Mie scattering phase functions can be input for each region.

3.1.4 Geometry

A description of an air-ground geometry is accomplished by dividing the geometry into regions bounded by horizontal plane surfaces

$$0 = COEE(NCB) - H \qquad 3.1.4.1$$

and/or right circular vertical cylindrical surfaces

$$0 = COEE(NCB) - R \quad , \qquad 3.1.4.2$$

where H and R are coordinates of a point on one of the surfaces, COEE(NCB) is the H intercept of the plane surface or the radius R of the cylindrical surface, and NCB is boundary number for a given surface. A region is defined by listing the numbers of the boundary surfaces encompassing the region. A plus or minus sign is affixed to each of the boundaries listed for a region to designate the boundary as an "upper" or "lower" plane surface or an "outer" or "inner" cylindrical surface with respect to the region being defined.

3.1.4.1 SEARCH Routine

In locating the region containing a particle's position H,R, the SEARCH routine calculates a value XR for each boundary encompassing the region by use of one of the equations

$$XR = COEE(NCB) - H$$

$$XR = COEE(NCB) - R$$

and compares the sign of XR with the sign affixed to the corresponding boundary number in the region input data. If the signs agree for all boundaries surrounding the region, then the point H,R is in the region under consideration. If not, then the SEARCH routine chooses the next region listed in the region table and repeats the process for that region. The SEARCH routine continues until all regions have been searched or until the region containing the point H,R has been located. The search is always begun with the most probable region of entry, MPR, for the last boundary that has been crossed. An error in listing the most probable region of entry will not result in an error in the calculations, but will increase the running time for a given problem.

3.1.4.2 Distance to a Boundary

The distance along the line of the particle's direction to a surface bounding the region is calculated in subroutine DSTBD. Subroutine DSTBD actually calculates the distances to all boundaries surrounding the region and takes the shortest positive distance as the distance traversed within the region. At any point a particle's position is given by the coordinates H,R and the direction is given by the two angles θ and ϕ. θ is the angle the particle's direction makes with the positive vertical vector and ϕ is the angle the projection of the particle's direction into a horizontal plane makes with the radial vector through the point H,R.

Distance to Plane Surface

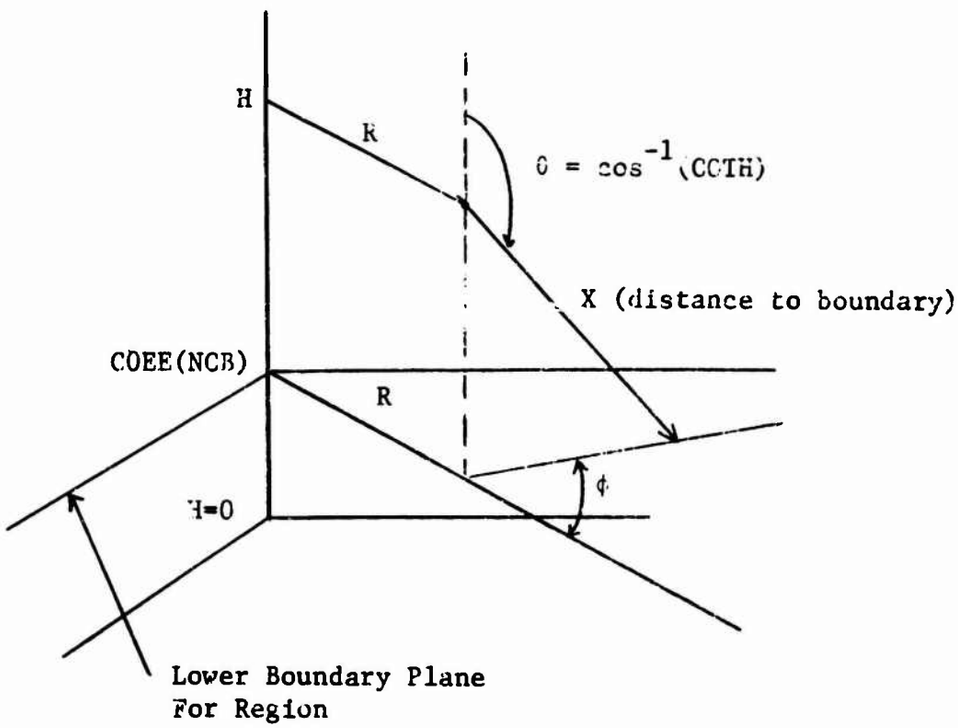

The distance X to a plane surface is calculated with the expression

$$X = (COEE(NCB) - H)/COTH,$$

where COEE(NCB) is the H intercept of the plane surface number NCB, and

COTH = $\cos\theta$ is the cosine of the angle between the particle's direction and the vertical vector.

The distance X to a cylindrical surface is given by the expression

$$X = \frac{-R*CPHI \pm \sqrt{COEE^2(NCB) - R^2*SPHI^2}}{SITH}$$

where COEE(NCB) is the radius of the cylindrical surface NCB,

CPHI and SPHI are the cosine and sine of the angle that the horizontal projection of the particle's direction makes with the radial vector through H,R, and

SITH is the sine of the angle the particle's direction makes with the vertical vector.

Distance To Cylindrical Surface

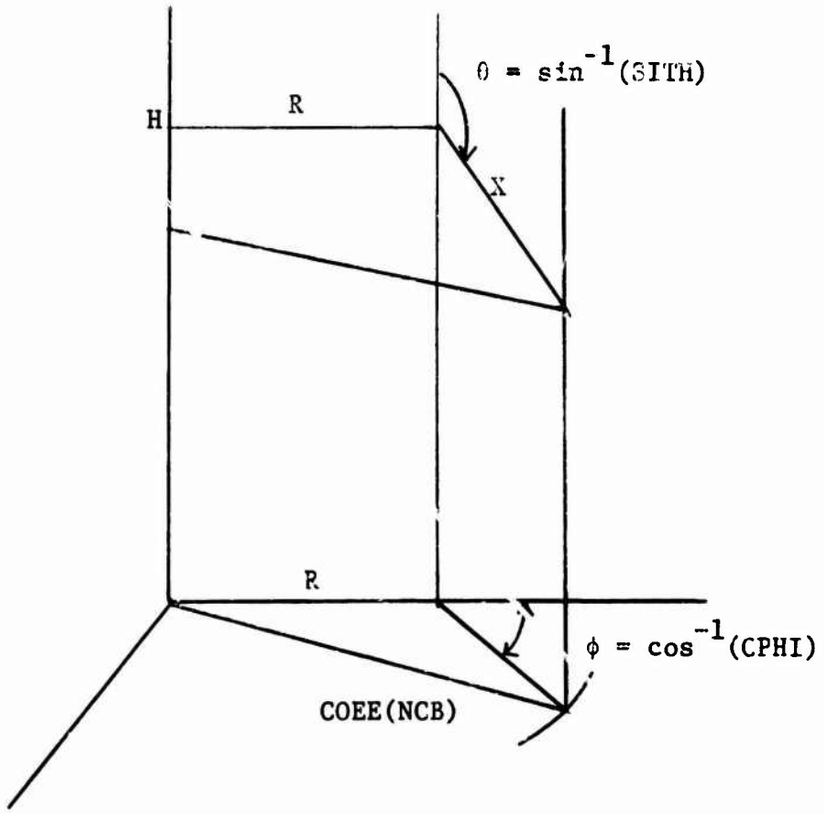

If the value under the radical is negative, then there is no intersection with the cylindrical surface NCB When the value under the radical is positive, the line intersects the cylindrical surfaces in two points. If the radical position of the point R is less than COEE(NCB), then the point H,R is inside the cylindrical surface and the positive radical is used to compute the distance X, but if the radial position of the point is greater than COEE(NCB), then the point H,R is outside the cylindrical surface and the negative radical is used to compute the distance X.

The distance DIST that a particle may travel within a region is initially set equal to the input value DLONG. Each time a distance X to a boundary surrounding the region is calculated, X is tested to determine whether it is a positive or negative quantity If X is negative, then DIST remains unchanged, but when X is positive, a comparison of X and DIST is made If DIST is less than X, then the value for DIST remains unchanged, but when DIST is greater than X, the value of DIST is set equal to X. After calculating the distances to all boundaries surrounding a region and performing the above tests, the final value of DIST should be the distance to the first boundary of intercept.

3.1.4.3 Region Importance Numbers

The region description provided by the LITE-I code not only allows for the input of different Mie scattering phase functions for each region of the atmosphere but it also allows the user to emphasize the sampling of collision points in those regions felt to be of most importance. Each region is assigned an importance number, EMP, in the problem input data As a light particle passes from one region to

another, the importance numbers of the two regions are compared. If the particle enters a region of the same or more importance, tracing of the particle is continued in a normal manner. If the particle enters a region of less importance, the ratio of the importance number of the region entered to the importance number of the previous region is compared with a random number. If the ratio is less than the random number, the particle is terminated. If the ratio is greater than the random number, the particle weight is divided by the ratio and tracing of the particle is continued. This method makes it possible to concentrate the sampling of particle collisions in those regions that contribute most significantly to the scattered intensity at the receiver positions. If a region is assigned an importance number of zero, then the particle histories for all particles entering that region will be terminated.

3.1.5 Statistical Estimation

The LITE-I code uses Monte Carlo methods to generate a random walk that gives the location of a particle's collisions within an air-ground geometry. A statistical estimation process is applied to predict the light intensity that scatters from each collision point of a random walk to each of a set of from one to ten point detectors. Since only the height and radius of each collision point are preserved to identify its location, the azimuthal position ϕ_D of the detector point is allowed to vary with each individual estimate to account for the three dimensional collision distribution. The code presently selects the azimuthal position ϕ_D of the detector

point from a uniform distribution between 0 and 2π, which, in effect, restricts the source angular distribution to one that is symmetrical about the vertical axis. The collisions are all assumed to lie on the $\phi_D = 0$ plane and the angle ϕ_D between the collision plane and the radius through the detector point is chosen with a rejection technique.

Geometry For Calculation of Flux at a Detector Point

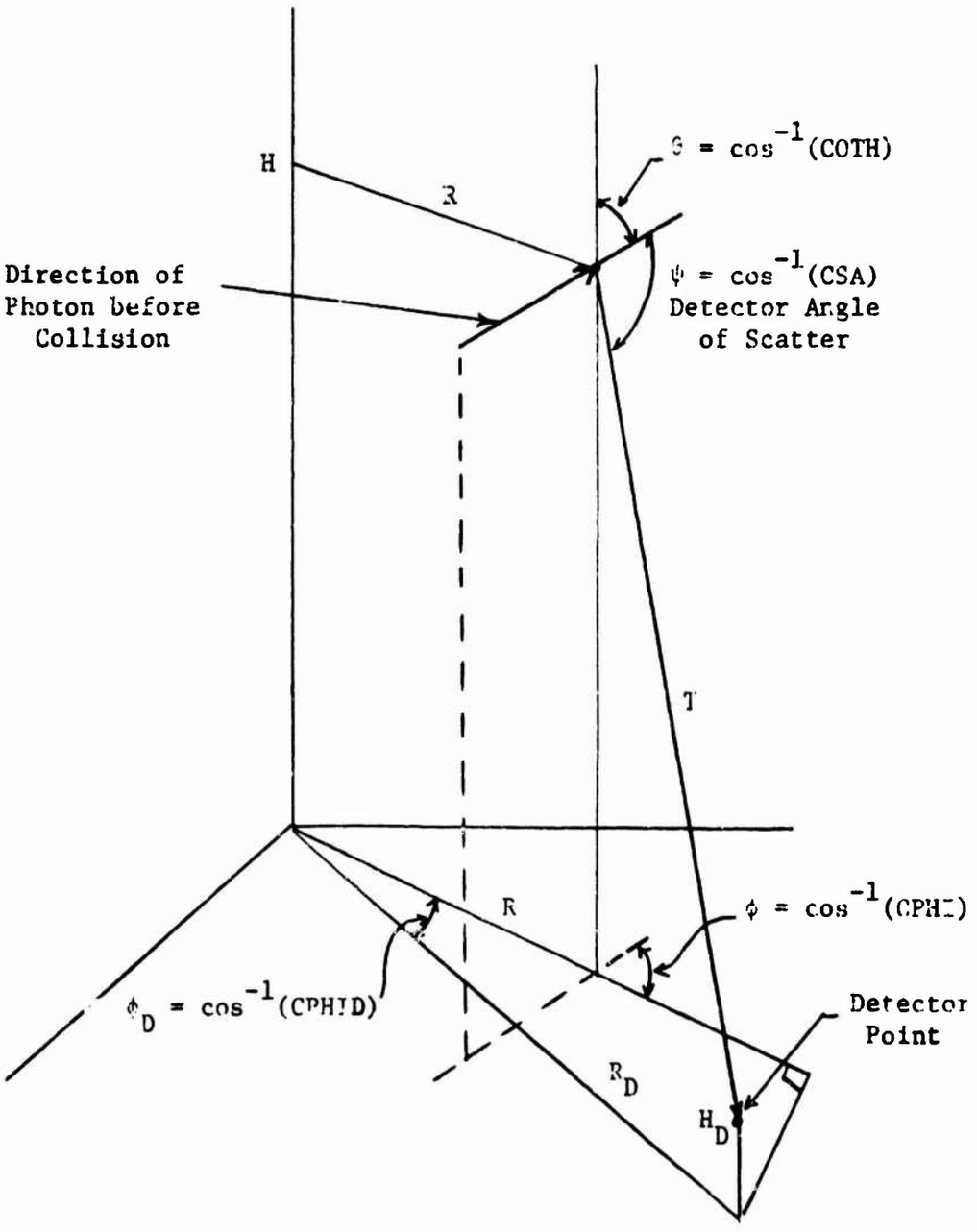

3.1.5.1 Detector Angle of Scatter

The cosine CSA of the angle between the particle's direction before collision and the line joining the collision and detector points is computed by taking the dot product of the two unit vectors in those directions. The unit vector in the particle's direction is

$$\hat{P} = (SITH*CPHI)\hat{i} + (SITH*SPHI)\hat{j} + (COTH)\hat{k}$$

where SITH and COTH are the sine and cosine of the angle between the particle's direction and the H axis, and

SPHI and CPHI are the sine and cosine of the angle between the horizontal projection of the particle's direction and the radial vector through the point of collision.

The unit vector in the direction of the line joining the collision and detector points is

$$\hat{D} = \left(\frac{R_D*CPHID - R}{T}\right)\hat{i} + \left(\frac{R_D*SPHID}{T}\right)\hat{j} + \left(\frac{H_D - H}{T}\right)\hat{k} \quad ,$$

where SPHID and CPHID are the sine and cosine of the detector's azimuthal angle,

R_D and H_D are the radius and height of the detector point,

R and H are the radius and height of the collision point.

The distance T from the collision point to the detector point is computed by use of the expression

$$T = \sqrt{R^2 + R_D^2 - 2RR_D\cos\phi_D + (H - H_D)^2} \quad .$$

CSA is then determined by the dot product $\hat{P}\cdot\hat{D}$.

3.1.5.2 Probability of Scattering Toward a Detector

CSA is the cosine of the angle through which a light particle must scatter in order to be directed toward the detector. Subroutine DIFSCA computes the probability of scattering within a unit solid angle about the angle whose cosine is CSA. Two different methods are used to compute the Rayleigh and Mie scattering probabilities. To determine the mode of scattering a random number is generated and compared to the value input for RAYR(H1), which is the ratio of the Rayleigh to the total scattering cross section at the altitude H1 of the collision point. When the random number is less than the value for RAYR(H1) (Rayleigh scattering occurs), the probability of scattering through an angle whose cosine is CSA is given by the expression

$$\text{PSCAT} = \frac{3}{16\pi} (1.0 + \text{CSA}^2) .$$

When the random number is greater than the value of RAYR(H1), the probability PSCAT is chosen from the input Mie scattering phase function for the region NCM containing the collision point. The interval containing the cosine value CSA is located and a linear interpolation between the two input values of PDCOS(NCM,J) corresponding to the two cosine values DIFCOS(NCM,J) that bound the interval is performed to obtain the value PSCAT for the cosine CSA.

3.1.5.3 Contribution From A Single Collision

The attenuation of the light scattered from a collision point to a detector point is determined by calculating the number of path lengths RHOT traversed along the line joining the collision and

detector point. RHOT is computed by use of the equation

$$RHOT = (TAUHD - TAUH2)\cos\theta$$

where TAUH2 is the collision altitude in mean-free-path lengths,

TAUHD is the detector altitude in mean-free-path lengths, and

$\cos\theta$ is the cosine of the angle between the line joining the collision and detector point and the positive vertical vector.

The contribution to the light intensity from a single collision is given by the expression

$$RESULT = (WAIT*PSCAT*e^{-RHOT})/T^2$$

where WAIT is the particle weight before scattering,

PSCAT is the probability of scattering into a unit solid angle about the direction toward the detector,

RHOT is the number of path lengths between the collision and detector points, and

T is the distance from the collision to the detector point.

3.1.6 Light Scattering

Each individual scattering event is assumed to be either Rayleigh or Mie scattering. For a given atmosphere the ratio of the Rayleigh to the total scattering cross section RAYR(hl) is input as a function of altitude where the hl are fixed heights in the atmosphere. The scattering process is selected by comparing a random number with RAYR(h), where RAYR(h) is found by interpolation between the RAYR(hl) values. When the random number is less than RAYR(h), the routine for Rayleigh scattering is used to select the scattering angle. Otherwise the Mie scattering routine is used.

3.1.6.1 Rayleigh Scattering

Rejection techniques are used to sample the polar and azimuthal scattering angles from the Rayleigh phase function which is expressed by the formulae

$$P(\Omega) = \frac{3}{16\pi} (1 + \cos^2\theta)d\Omega \qquad 3.1.6.1$$

where $d\Omega = \sin\theta d\theta d\phi$.

Equation 3.1.6.1 is expressed as the product of two probability density functions, $\frac{d\phi}{2\pi}$ times $\frac{3}{8} (1 + \cos^2\theta)\sin\theta d\theta$. The azimuthal angle of scatter is selected from the probability density function

$$P(\phi) = \frac{d\phi}{2\pi}$$

and the polar angle θ is selected from the probability density function,

$$P(\cos\theta) = \frac{3}{8} (1 + \cos^2\theta)\sin\theta d\theta \ .$$

Selection of the azimuthal angle is accomplished by use of the following well-known rejection technique. An X is chosen from a uniform distribution in the interval $-1 \leq X \leq 1$ by use of the equation

$$X = 2*RN_1-1,$$

and a Y is chosen from the same distribution by use of the equation

$$Y = 2*RN_2-1,$$

where RN_1 and RN_2 are random numbers. If the point X, Y lies outside a circle with unit radius, then two more values of X and Y are chosen and the process is repeated until a point X, Y is found within the circle. The sign and cosine of the azimuthal scattering angle are then given by the equations

$$\cos\theta = \frac{X}{\sqrt{X^2+ Y^2}}$$

$$\sin\theta = \frac{Y}{\sqrt{X^2+ Y^2}}.$$

A rejection technique was developed to select a polar angle θ from the probability density function,

$$P(\cos\theta) = \frac{3}{8} \quad (1 + \cos^2\theta)\sin\theta d\theta \ .$$

For this technique the above density function is expressed as the sum of two probability density functions

$$P(\cos\theta) = P_1(\cos\theta) + P_2(\cos\theta)$$

where $P_1(\cos\theta) = \frac{3}{4} \frac{\sin\theta d\theta}{2}$

$$P_2(\cos\theta) = \frac{3}{4} \cos^2\theta \frac{\sin\theta d\theta}{2} \ .$$

The density function $P_1(\cos\theta)$ is chosen to represent the polar angular distribution (3/4)/(6/4) or $\frac{1}{2}$ of the time, and the density function $P_2(\cos\theta)$ is chosen the remainder of the time. If the density function $P_1(\cos\theta)$ is chosen, then $\cos\theta$ is determined by solving the integral,

$$RN = \int_0^{\theta_p} \frac{\sin\theta d\theta}{2}$$

for $\cos\theta_p$.

Thus $\cos\theta_p = 1-2*RN$.

When the density function $P_2(\cos\theta)$ is chosen, $\cos\theta_p$ is again computed by the above expression, but the value of $\cos\theta_p$ is not accepted unless a second random number is less than $\cos^2\theta_p$. If $\cos\theta_p$ is not accepted, then the process of selecting a density function and computing a value of $\cos\theta_p$ is repeated until either $P_1(\cos\theta)$ has been used to obtain a value of $\cos\theta_p$ or $P_2(\cos\theta)$ has been used and the value has been accepted. The expected number of trials before accepting a $\cos\theta_p$ is 3/2 and the efficiency of the technique is 2/3.

A FORTRAN code was prepared for the purpose of verifying the accuracy of the rejection technique described above. The printout of

the code gives the number of angles sampled within each .05 interval of cosθ between 1 and -1. Figure 7 shows a comparison of the cumulative distribution of the scattering angles sampled with the code and the cumulative Rayleigh phase function. The good agreement between the two curves indicates the rejection technique does properly sample scattering angles from the Rayleigh phase function.

3.1.6.2 Mie Scattering

The azimuthal angle for the Mie scattering process is chosen in the same manner as that described for Rayleigh scattering. The Mie scattering polar angle is selected from the input cumulative Mie scattering angular distribution. For each region J there are NPHANG(J) cosine values, PHANG(J,I), input corresponding to equal intervals of the accumulative Mie scattering angular distribution. A random number is generated and the values I-1 and I determined such that

$$(I-1)/NPHANG(J) \leq RN \leq I/NPHANG(J).$$

$Cos\theta_p$ is then determined by a linear interpolation between the cosine values PHANG(J,I-1) and PHANG(J,I) to give the cosine of the angle corresponding to the random number.

3.1.6.3 Direction after Collision

The light particle's direction after scatter is determined from a knowledge of its direction before scattering and the polar and azimuthal angles of scatter. The cosine of the particle's direction after scatter, COTH1, is given by the equation,

COTH1 = COTH2*CSANG+SITH2*SSANG*CDPHI,

where COTH1 is the cosine of the angle between the particle's direction after scatter and the vertical axis,

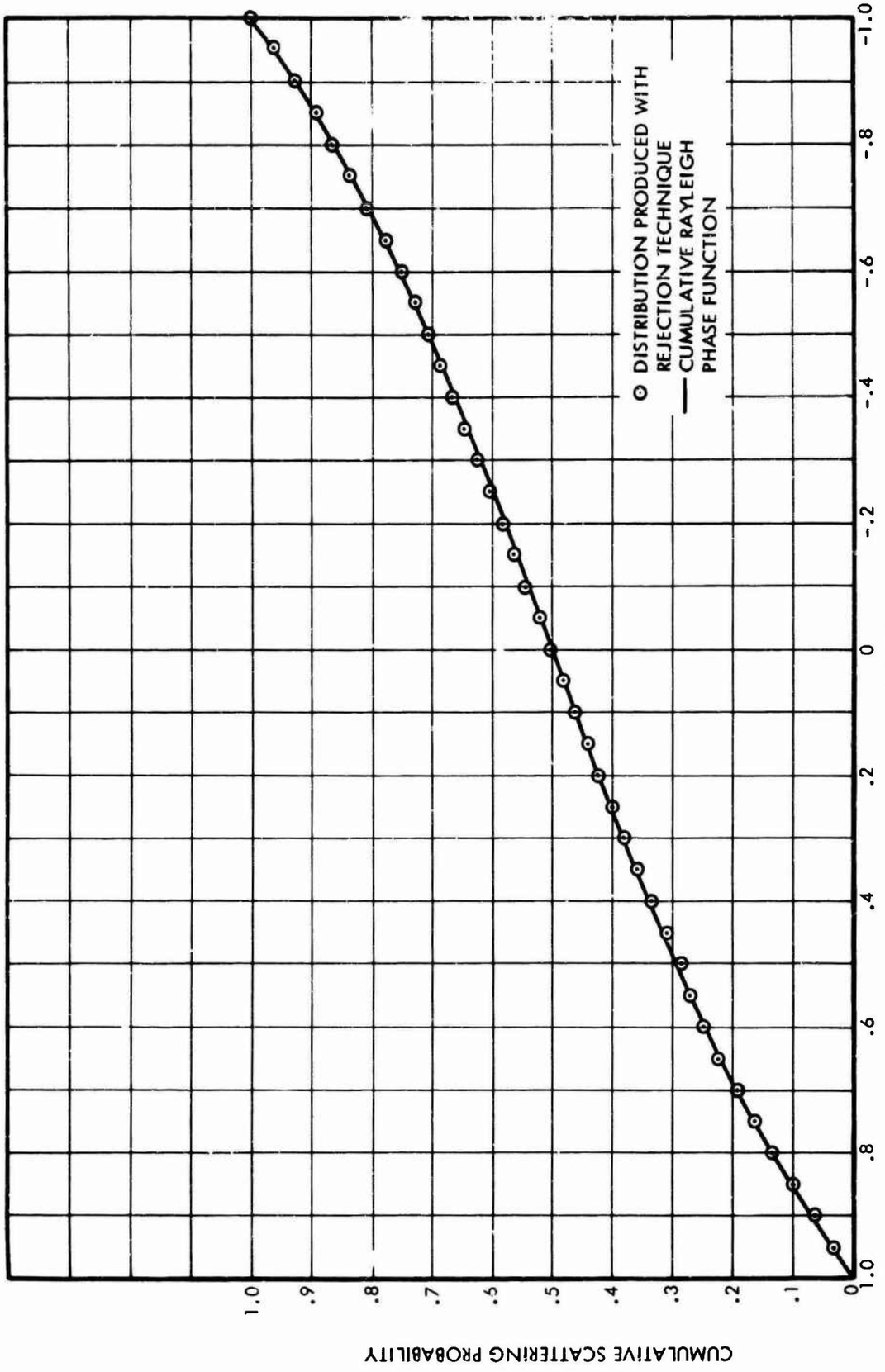

Fig. 7. Comparison of Cumulative Distribution of Angles Sampled Using Rejection Technique with Cumulative Rayleigh Phase Function

SITH2 and COTH2 are the sine and cosine of the angle between the particle's direction before scattering and the vertical axis, SSANG and CSANG are the sine and cosine of the polar angle of scatter, and CDPHI is the cosine of the azimuthal angle of scatter.

Geometry for Calculation of Direction After Collision

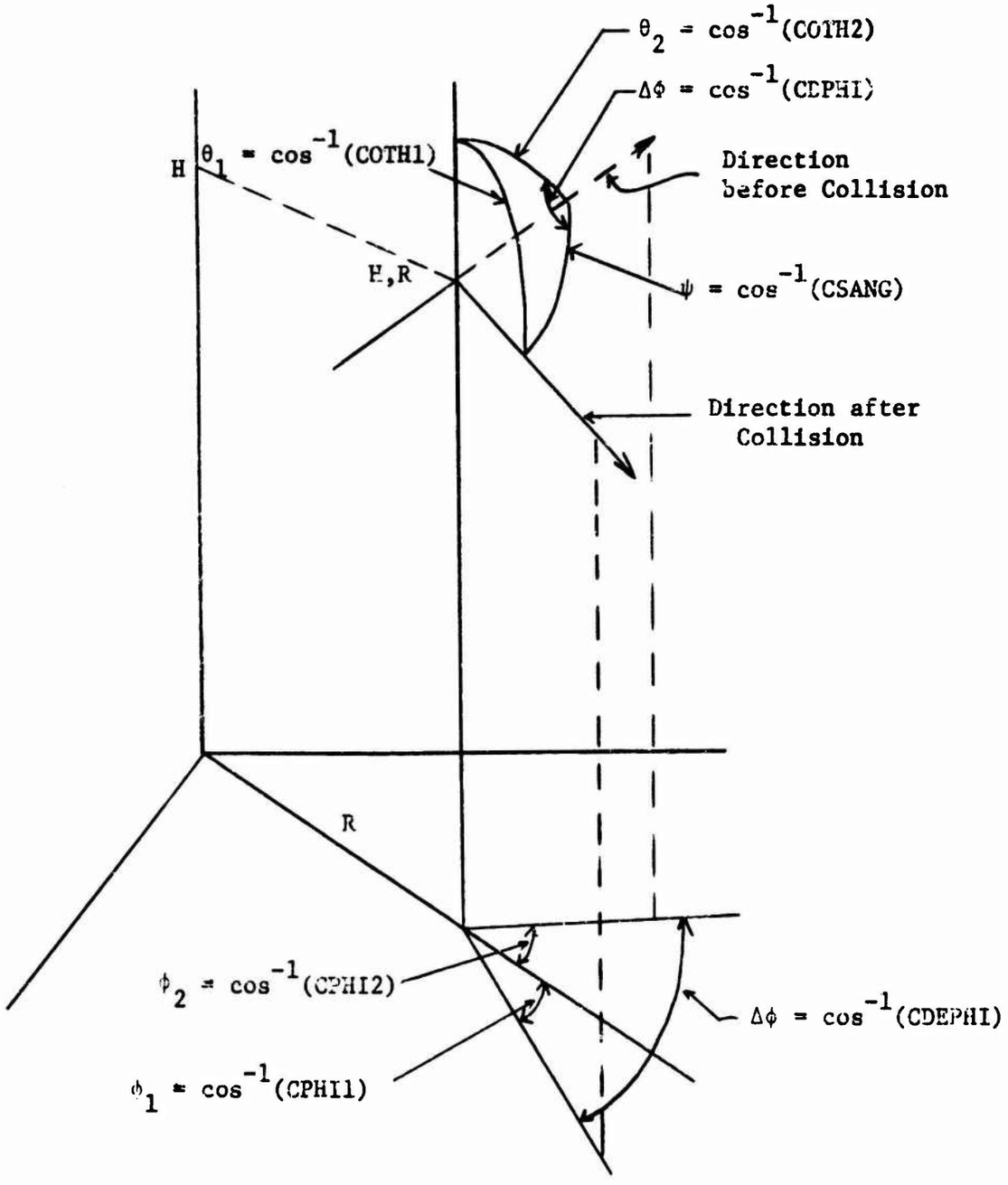

The sine of the angle between the particle's direction after scattering and the vertical axis is given by

$$SITH1 = \sqrt{1.0 - COTH1^2} \quad .$$

The sine and cosine of the angle between the horizontal projection of the particle's direction after scattering and the radial vector through the collision point are given by the equations

SPHI1 = SPHI2*CDEPHI + CPHI2*SDEPHI, and

CPHI1 = CPHI2*CDEPHI-SPHI2*SDEPHI,

where SPHI2 and CPHI2 are the sine and cosine of the angle between the horizontal projection of the particle's direction before scattering and the radial vector through the scattering point,

SDEPHI = SSANG*SDPHI/SITH1, and

CDEPHI = (CSANG - COTH1*COTH2)/SITH1*SITH2 .

3.1.7 Ground and Cloud Reflections

Light reflection from the ground and cloud surfaces can be treated with an albedo method. If the albedo method is to be used, then the reflection surfaces are listed first in the boundary table of the LITE-I input and are identified by the negative sign preceding the boundary number NBOUND. The value assigned to the parameter ALBEDO(NCB) gives the fraction of the incident photon current that is reflected from the surface NCB and the value input for the parameter JREFLT(NCB) determines the angular distribution of the albedo. The angular distribution is taken to be isotropic or anisotropic in the upper hemisphere if JREFLT(NCB) is 1 or 2, or isotropic or anisotropic in the lower hemisphere if JREFLT(NCB) is 3 or 4. When reflection is isotropic,

in either the upper or lower hemisphere, no input reflection distributions are required. If reflection is anisotropic, then values must be input to define both the reflection distribution and the cumulative reflection distribution.

3.1.7.1 Reflection Into A Detector

The code treats light reflection from a surface as if the point of reflection is a scattering center at the reflection surface. The probability of scattering toward the detector and the angle of scatter is determined from the reflection distributions rather than from Rayleigh or Mie scattering distributions. The input reflection distributions are defined about the normal to the reflection surface.

Reflection into Detector

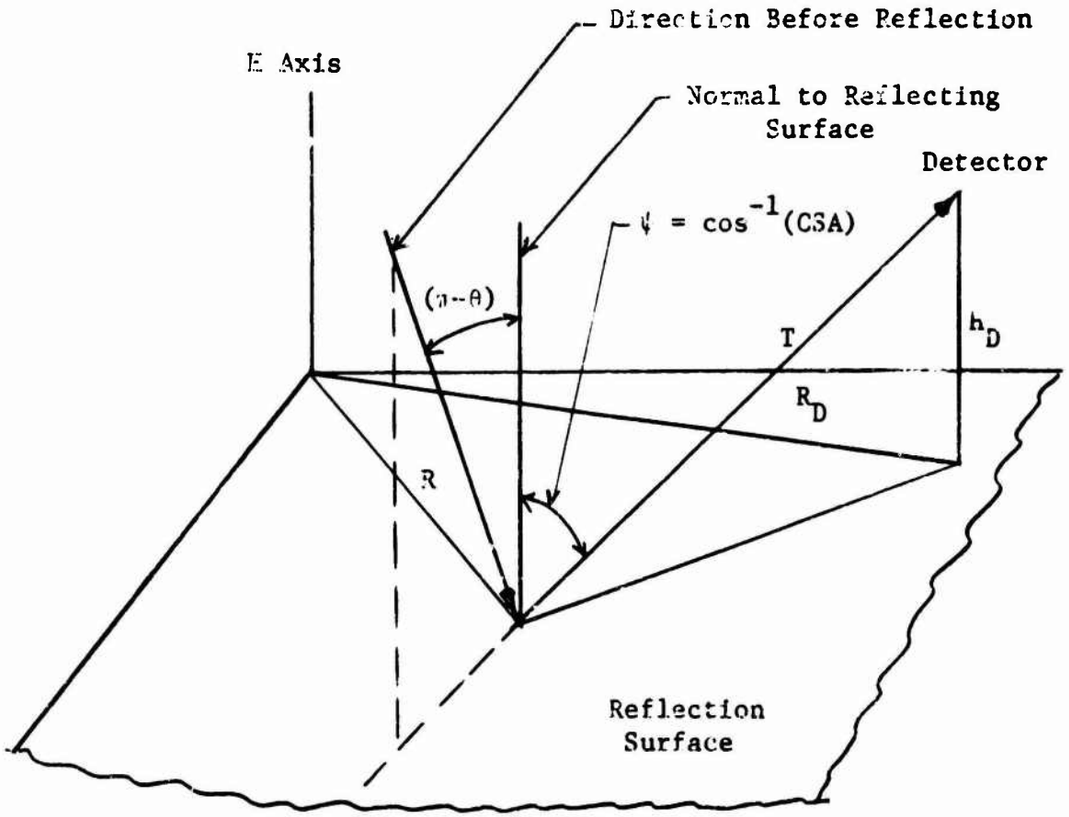

The input values POR(NRB,J) define an anisotropic reflection distribution for the cosine values RFANG(NRB,J) for the reflection surface NRB. For anisotropic reflection the probability, PSCAT, of light reflecting from a surface into a unit solid angle toward a detector is determined by calculating the cosine, CSA, of the angle between the line joining the scattering center to the detector and the normal to the surface, and then evaluating the probability of light reflecting at that angle by a linear interpolation between the two values of POR(NRB,J) corresponding to the values of RFANG(NRB,J) that bound the interval containing CSA. The angular distribution of the current reflected from a surface is assumed to be dependent only on the polar angle of reflection and to not vary with the azimuthal angle for any given polar angle.

For isotropic reflection in the upper or lower hemisphere the probability, PSCAT, of light reflecting into a unit solid angle toward the detector is taken by the code to be $1/2\pi$.

The light intensity reflected into the detector from the scattering center is given by the expression,

$$\text{RESULT} = \text{WAIT}*\text{ALBEDO(NRB)}*\text{PSCAT}*e^{-\text{RHOT}/T^2}$$

where RESULT is the contribution to the light intensity from the scattering center at the reflection surface,

WAIT is the light particle weight before scattering,

ALBEDO(NRB) is the fraction of the particle that is reflected from the surface NRB,

PSCAT is the probability of the particle being reflected into a unit solid angle toward the detector,

RHOT is the number of optical path lengths between the scattering center and the detector, and

T is the distance between the scattering center and the detector.

3.1.7.2 Reflection Angle

After computing the light intensity reflected to the detector, a reflection angle is chosen from the cumulative reflection distribution in order to trace the light particle to the next collision point. If reflection is isotropic, then the cosine of the scattering angle is given by the expression CSA = RN for reflection into the upper hemisphere and by the expression CSA = -RN for reflection into the lower hemisphere, where RN is a random number.

When reflection is anisotropic, the scattering angle CSA is selected from the NRFCOS(NRB) cosine values, RFLCOS(NRB,I), input for equal intervals of the cumulative reflection distributions. A random number is generated and the values I-1 and I determined such that

$$(I-1)/NRFCOS(NRB) \leq RN < I/NRFCOS(NRB).$$

The cosine of the reflection angle is then calculated by interpolating between the two cosine values RFLCOS(NRB,I-1) and RFLCOS(NRB,I) to give a cosine corresponding to the random number.

3.1.8 Printout of Scattered Intensities

As discussed previously in this section the scattered light intensity as calculated with the LITE-I code is printed in several different formats. The scattered intensity is given as a function

of the order of collision at each receiver position so that the effect of multiple collisions may be analyzed. In addition, the angular distribution of the scattered intensity is printed as a function of the order of reflection from the first reflection surface listed in the problem input data. Thus the intensities listed for the zero order of reflection include the estimates of the light intensity from all collisions that occur before a light particle intersects the first reflection surface. The intensities listed for the first order of reflection include those estimates of the light intensity reflected into a receiver due to the first reflection and the estimates of the intensity from all those collisions that occur in the atmosphere after the particle has one reflection and before it is reflected a second time.

The printout of the scattered intensity as a function of the order of reflection allows one to use the results for a problem run with one ground or cloud albedo to predict the intensity for a problem in which all other parameters remain the same except the ground or cloud albedo. This allows a determination of the effect of varying the ground or cloud albedo with only one computer run. To convert the printout from one albedo to another, the intensities listed for the nth order of reflection should be multiplied by the ratio

$$(\text{ALBEDO}'/\text{ALBEDO})^n$$

where ALBEDO is the albedo used to obtain the printout,

ALBEDO' is the albedo for which the intensities are desired, and

n is the order of reflection.

After multiplying the intensities listed for each order of reflection by the above ratios, the products may be summed over all orders of reflection to give the total intensity for the problem with the albedo ALBEDO'. If the above method is to be used to study the effect of varying the ground or cloud albedo, it would be advisable to run the initial problem for the highest albedo to be considered.

The scattered intensities are also printed as a function of the region of scatter for each receiver point to determine those regions of the atmosphere in which the scattering is most significant. Thus, if a series of similar problems are to be run, the first problems may be used to designate the more important regions of scatter and those regions may be emphasized in later problems by assigning those regions a higher importance number.

3.1.9 Direct Intensity Calculation

The direct intensity at each receiver point is calculated with the equation

$$DI(J) = DBSS(J)e^{\frac{-(TAUHD(J) - TAUHS)/\cos\theta}{T^2}}$$

where DI(J) is the direct intensity at the Jth receiver position,

DBSS(J) is the number of light particles per unit solid angle emitted from the source in the direction toward the Jth receiver per unit source strength,

TAUHD(J) is the height of the Jth detector in mean-free-path lengths,

TAUHS is the source height in mean-free-path lengths,

$\cos\theta$ is the cosine of the angle between the line joining the source and receiver points and the vertical vector, and

T is the distance from the source to the receiver point.

When the source is isotropic, DBSS(J) = $1/4\pi$ for all receiver points. If the source is anisotropic, then

$$DBSS(J) = \frac{PAG(I) - PAG(I-1)}{2\pi|CANG(I) - CANG(I-1)|}$$

where $CANG(I) \leq \cos\theta < CANG(I-1)$ and PAG(I) is the probability that a particle will be emitted from the source in the polar angle interval 0° to $\cos^{-1}(CANG(I))$.

3.2 Description of the LITE-II Code

The methods used in the LITE-II code to treat the source angular distribution and biasing of the source angular distribution are the same as the methods previously described for the LITE-I code, except that the angular distribution data input to the LITE-II code are for a plane source rather than a point source. Thus it is possible to treat plane sources with an arbitrary angular distribution located at the top of the atmosphere or anywhere within the atmosphere.

The methods used to select random optical path lengths between collisions in the LITE-II code are the same as those described in Section 3.1 for the LITE-I code. The cross section input data and geometry description for the LITE-II code also correspond to that used in the LITE-I code.

The major difference between the two codes is in the methods used to estimate the scattered intensity at the receiver positions. In the LITE-II code, estimates of the scattered intensity at plane

receivers are made rather than at point receiv[illegible] Through the use of the reciprocity principle, the estimates of t[illegible] intensity from a point source at infinite plane receivers are applied to predict the intensity at point receivers due to an infinite plane source.

In the LITE-II code a new particle direction after each collision is chosen from either the Rayleigh or Mie scattering phase function as discussed in Section 3.1.2. Then an estimate of the light intensity reaching each of the receiver planes that intersect the particle's positive directional vector is made. The estimate of the intensity at a receiver plane is given by the equation,

$$RESULT = (WAIT * e^{-RHOT}) / |\cos\theta|$$

where WAIT is the particle weight after collision,

RHOT is the number of mean-free-path lengths between the collision point and receiver plane along the particle's directional vector, and

$\cos\theta$ is the angle between the particle's directional vector and the positive vertical vector.

In the LITE-II code the estimates of the intensity at each receiver plane are stored and later printed as a function of the cosine of the angle between the particle's direction as it crosses the receiver plane and the normal to the plane.

The equation used to calculate the direct intensity in the LITE-II code is the same as that used for the LITE-1 code. However, the equation can be made to apply to plane parallel sources by inputting the proper value for DBSS(J). In order for the direct-beam calculation given by the equation,

$$DI(J) = DBSS(J)\ e^{-(TAUHD(J) - TAUHS)/\cos\theta} / T^2 ,$$

to apply to a plane parallel source, the values RD(J) input for the radial positions of the receiver positions should be determined by the expression

$$RD(J) = (HD(J) - HS)/\cos\theta$$

where HD(J) is the vertical position of the receiver plane,

HS is the vertical position of the source, and

$\cos\theta$ is the cosine of the angle that plane parallel source makes with the vertical vector.

In addition, the values input for DBSS(J) should be the number of source photons incident per unit area upon the atmosphere times the secant of the incident angle times the square of the slant distance T^2 between the source and receiver positions, that is, $DBSS(J) = T^2\sec\theta$ for a source strength of one particle per unit area on top of the atmosphere.

In the special case where the plane source has an input angular distribution defined by the parameters PAG(J) and CANG(J), then the direct-beam intensity at the Ith detector plane per photon incident per unit area of the source can not be evaluated by the code. It can, however, be computed separate from the Monte Carlo calculations by use of the expression

$$DI(I) = 2\pi \int_0^{2\pi} G(\theta) e^{-\tau(I)\sec\theta} \tan\theta d\theta$$

where $\tau(I) = TAUHD(I) - TAUHS$,

$$G(\theta) = \frac{PAG(J) - PAG(J-1)}{2\pi(CANG(J-1) - CANG(J))} \quad \text{for}$$

$$CANG(J) < \cos\theta \leq CANG(J-1) .$$

The function $G(\theta)$ defines the number of source particles per unit area of the source plane that are moving per unit solid angle in the direction θ, where θ is the source polar angle measured from the vertical H axis. When the radiation incident on the top of the atmosphere is isotropic, then $G(\theta) = \frac{1}{2\pi}$. If the plane source is located within the atmosphere and is isotropic in all directions, then $G(\theta) = \frac{1}{4\pi}$.

IV. COMPARISONS WITH LITE CODE RESULTS

In order to insure that the LITE code calculates properly the intensity of scattered light, several test problems have been run to compare with other calculations. Calculated, rather than experimental data, were chosen to validate the LITE codes, since in most cases, input information for the calculated results are much better defined than are the atmospheric and terrain conditions under which the experimental data were taken. Although some of the calculated data chosen for this purpose do not pertain to light transport in the atmosphere, the scattering mechanisms involved in the calculational methods are the same as those used in the LITE codes.

4.2 LITE-I Code Results

Calculations were made using the K74 Monte Carlo transport code to determine the direct and scattered intensity as a function of distance from a point isotropic source in an infinite media for comparison with similar results obtained from the LITE-I code.

Figure 8 shows the comparison of the LITE-I code results with the K74 code results for a .45 micron wave length point isotropic source embedded with an infinite air medium in which the aerosol size distribution was taken to be proportional to $1/r^3$, and the ratio of Rayleigh to total scattering cross section was taken to be 0.58. Results for problems run with the ALGOL version of the LITE-I code are shown. The LITE-I code calculated intensities for point receivers located a distance R from the source were multiplied by $4\pi R^2$, since this was the form of the K74 results. These data are for ten orders

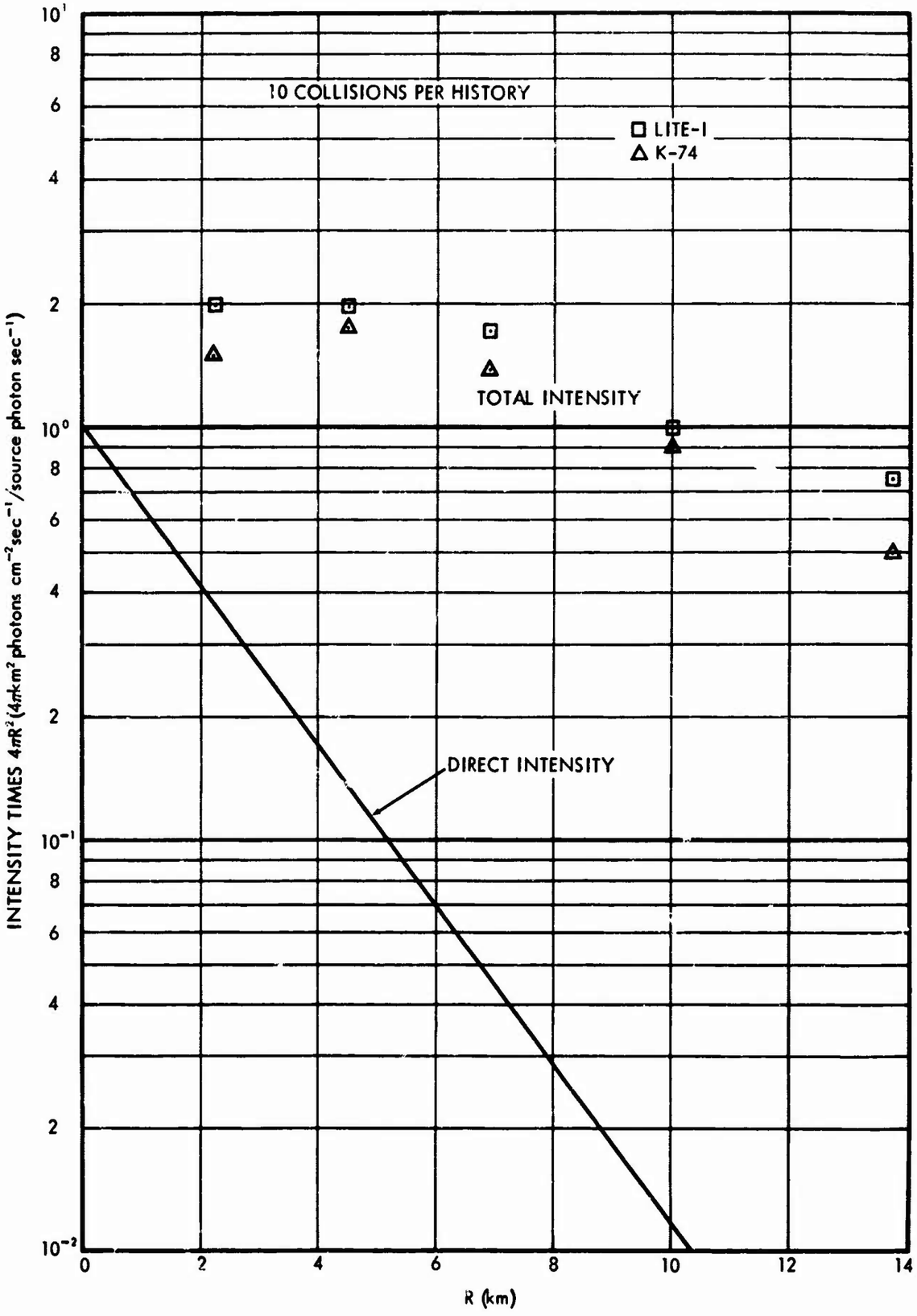

Fig. 8. Comparison of LITE-I Code and K-74 Results for an Infinite Medium

of scattering which does not represent the total scattered intensity in this case, because in an infinite media, orders of scattering above twenty would still contribute significantly to the total scattered intensity.

Several LITE-I code problems were run to compare with Coulson, Dave, and Sekera's calculations of the radiation emerging from a planetary atmosphere with Rayleigh scattering (Reference 10). Coulson's data were for plane monodirectional sources incident upon the top of the atmosphere. In order to compare the LITE-I code results with the plane source data, the scattered intensities $I(\tau,\alpha,\rho)$ as a function of the radial distance from the vertical axis through a point monodirectional source were calculated, and these intensities were then integrated to give the results for a plane source. The radial distribution of the transmitted scattered intensity is denoted as $I(\tau,\alpha,\rho)$, where τ is the thickness of the atmosphere in mean-free-paths, α is the ground albedo, and ρ is the radial distance along the ground surface from the vertical axis through the source point. The integral

$$T(\tau,\alpha) = 2\pi \int_0^\infty \rho\, I(\tau,\alpha,\rho)\, d\rho$$

gives the scattered intensity transmitted through a planetary atmosphere of thickness τ mean-free-paths and ground albedo of α for a plane source incident on top of the atmosphere. Also of primary interest in running the LITE problems to compare with the data of Coulson *et al.*, was the effect of varying the extinction coefficient with altitude. To check the effect of varying the extinction coefficient with altitude, hand calculations were made of the single

scattered intensity transmitted through a Rayleigh atmosphere of 0.5 optical thickness in which the extinction coefficient was held constant with altitude and through a Rayleigh atmosphere of the same optical thickness in which the extinction coefficient was allowed to vary exponentially with altitude according to the expression

$$\Sigma(h) = 0.00625e^{-0.0125h} ,$$

where h is in arbitrary units.

The hand calculations are compared with the single-scattered intensities calculated with the LITE code in Figure 9. In both instances the agreement is very good. The variable density problem overpredicted the intensities for the constant density problem for detector points near the vertical axis and underpredicted the constant density results for detector points at the larger distances. Of significant interest is the fact that the integration of the results for the two cases over the lower plane of the atmosphere gives essentially the same results. Thus it would indicate that in situations involving the transmission of radiation through a slab geometry due to a plane source incident on the slab, only the optical thickness of the slab is of significance; but in situations involving a point source, the manner in which the extinction coefficient varies with altitude does affect the intensity at a distance, ρ, from the vertical axis through the source point.

Two LITE-I problems were run for a Rayleigh atmosphere of 0.13 optical thickness. For both problems, a monodirectional point source was incident normal to an atmosphere that decreased in density with increasing altitude. In the first problem the ground albedo was zero,

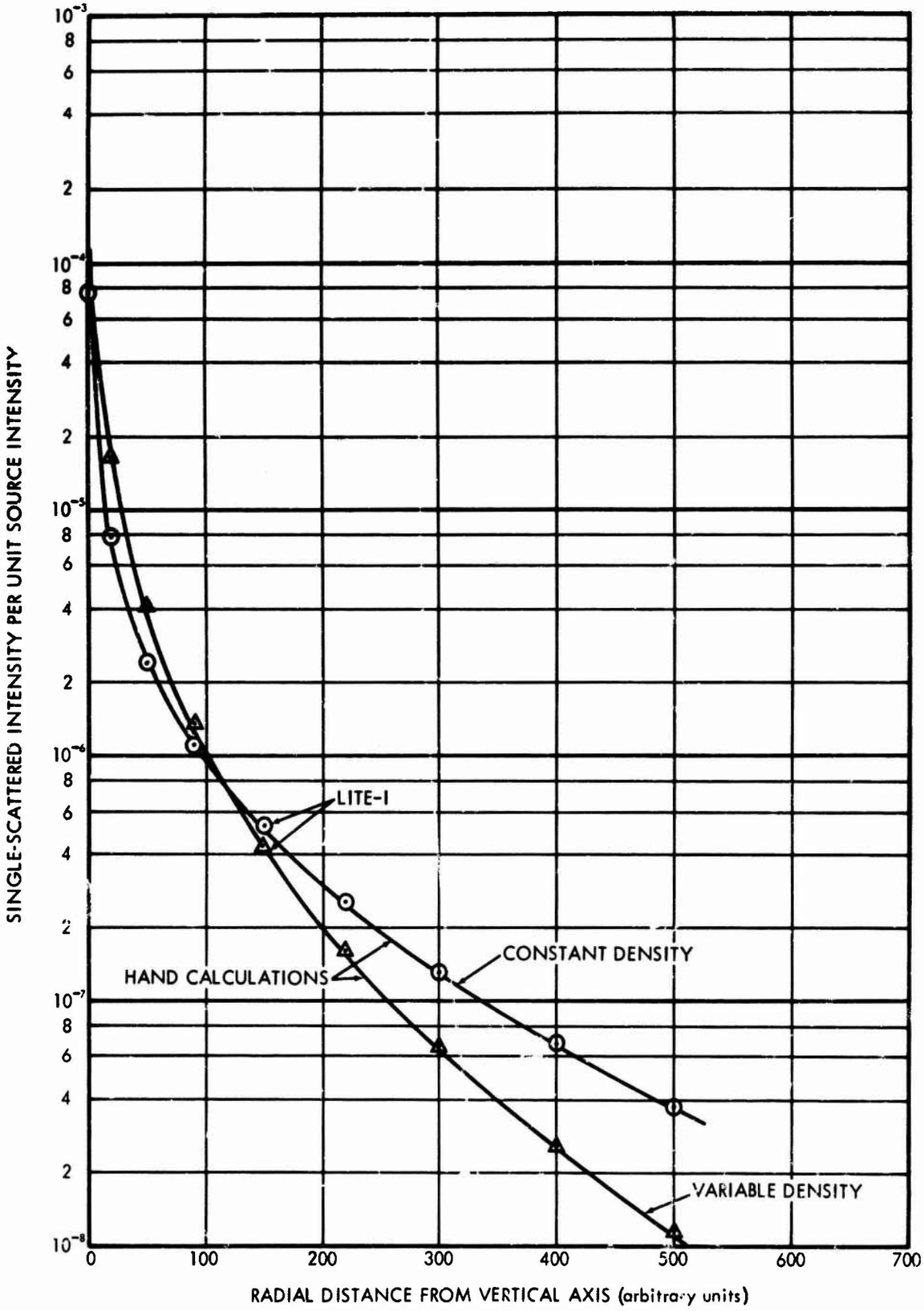

Fig. 9. Comparison of Hand-Calculated and LITE-I Code Single Scattered Intensities: $\tau = 0.5$, $\theta_o = 0^\circ$, Albedo = 0.0

and in the second problem the ground albedo was 0.8. The results of the two problems are shown in Figure 10. By integrating the results of the two problems over a plane surface, the transmitted intensities for a plane source incident normal to a 0 13 mean-free-path thick Rayleigh atmosphere were obtained for ground albedos of zero and 0.8. These transmitted intensities are compared with the transmitted intensities obtained from Coulson's data in Table II.

Table II. Scattered Light Transmitted Through Rayleigh Atmospheres for a Normal Incident Plane Parallel Broad Beam Source

τ	Air Density	Albedo	Scattered Intensity (photon cm^{-2}/source photon cm^{-2})	
			LITE Code	Coulson
0.5	Constant	0.0	0.405	0.403
0.5	Variable	0.0	0.358	0.403
0.5	Constant	0.8	0.964	1.032
0.5	Variable	0.8	1.06	1.032
0.13	Variable	0.0	0.160	0.1655
0.13	Variable	0.8	0.476	0.440

Also shown in Table II are the integrated intensities for two problems run for Rayleigh atmospheres of 0.5 optical thickness. One of the problems considered an atmosphere of constant density, and the other, a variable density atmosphere in which the extinction cross section varied exponentially with altitude according to the expression,

$$\Sigma(h) = 0.00625^{-0.0125h} .$$

In both problems the ground reflection distribution was input to conform to Lambert's law of reflection. The printout of the

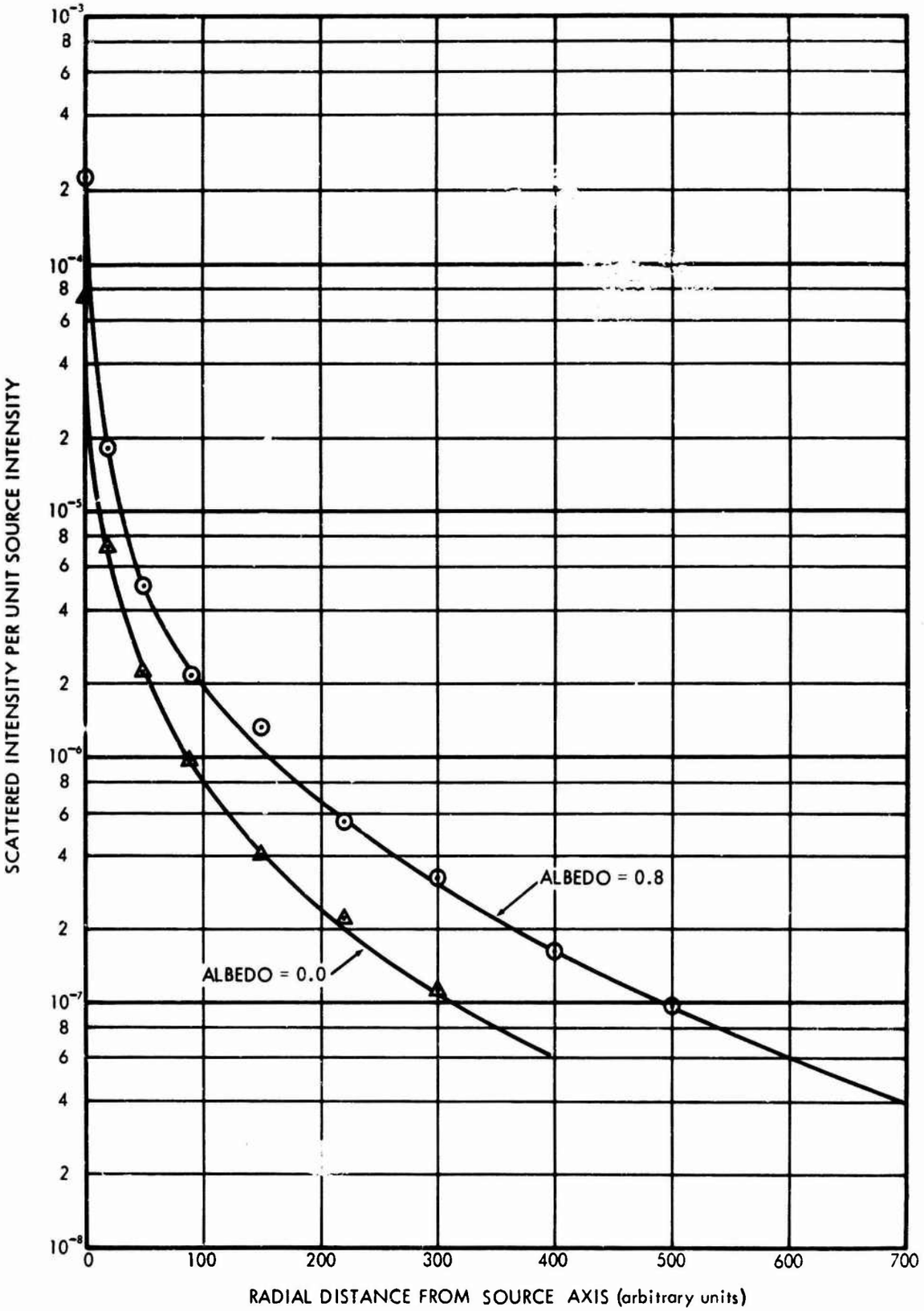

Fig. 10. Scattered Intensity Transmitted through a 0.13 Mean-Free-Path Thick Variable Density Rayleigh Atmosphere: Normal Incident Line Beam Source

scattered intensities as a function of the order of reflection for a ground albedo of 0.8 made it possible to determine the scattered intensities for a ground albedo of 0.0. The integrated intensities obtained in this manner for a ground albedo of 0.0 are also shown in Table II. The agreement between the LITE-I code data and Coulson's data is reasonably good for both the constant and variable density cases. There is a possibility of some error in integrating the LITE-I code data, because the spacing of the receiver points. The intensity as a function of radial position decreases very rapidly near the source axis and a slight shift of the radial distribution curve in this area can change the integrated intensity by as much as 10%. The sharp decrease can be observed in Figures 11 and 12, where radial distributions of the transmitted scattered intensities obtained with the two problems are shown.

The difference in the radial intensity of the multiple scattered radiation for the constant and variable density atmosphere is seen to follow the same pattern as did the radial intensities for the single scattered intensities. In each of the two problems plotted in Figures 11 and 12, a maximum of 20 collisions per history was allowed. The contributions from the 20th order of collision were a factor of approximately 10^3 to 10^5 lower than those from the first order of collision. Slightly more than one-half of the particles escaped out of the problem geometry before they had undergone 20 collisions.

Problems have also been run with the LITE-I code to produce results for comparison with exact solutions reported by Beach

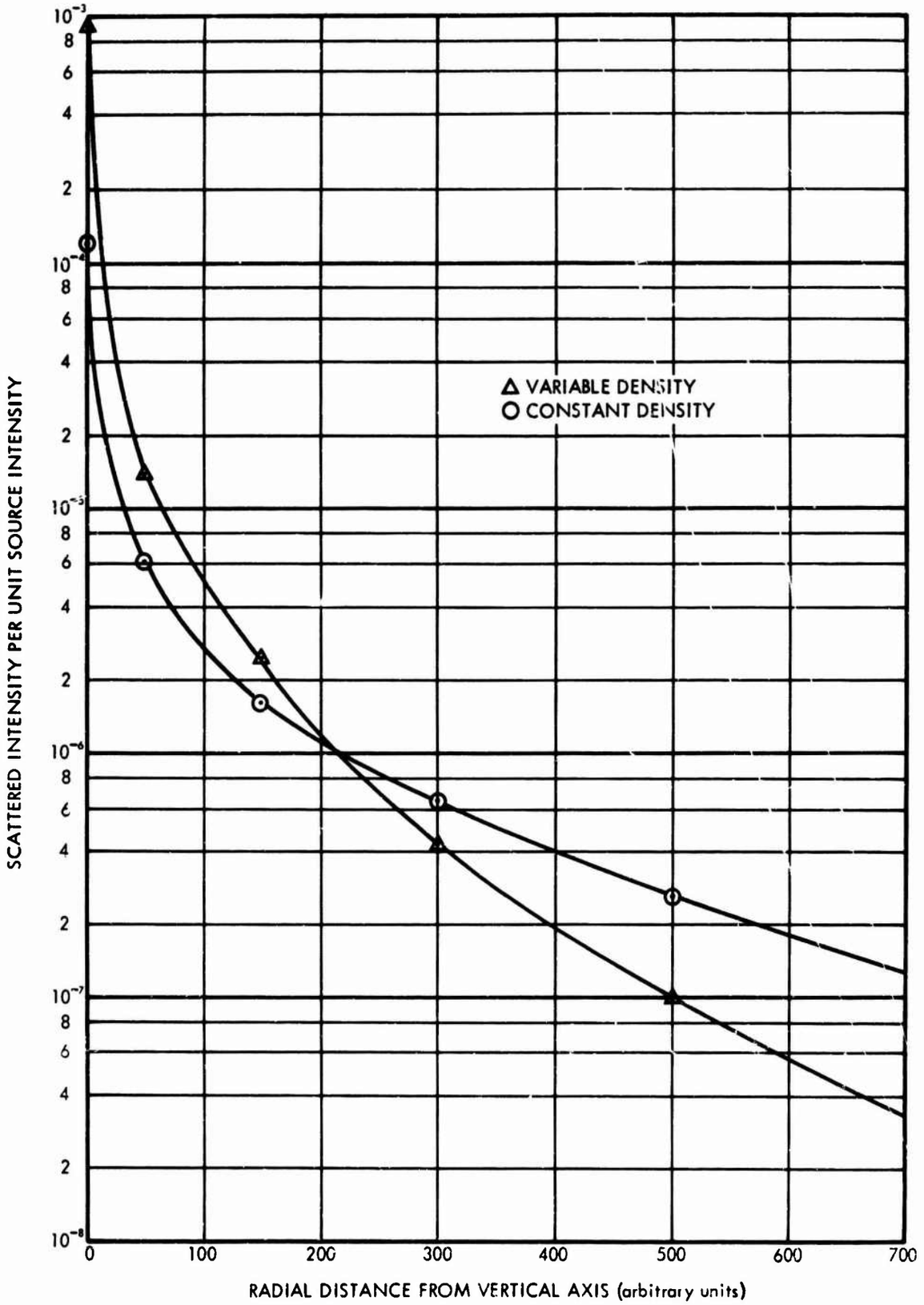

Fig. 11. Scattered Intensity Transmitted through a 0.5 Mean-Free-Path Thick Rayleigh Atmosphere: Normal Incident Line Beam Source, Albedo = 0.8

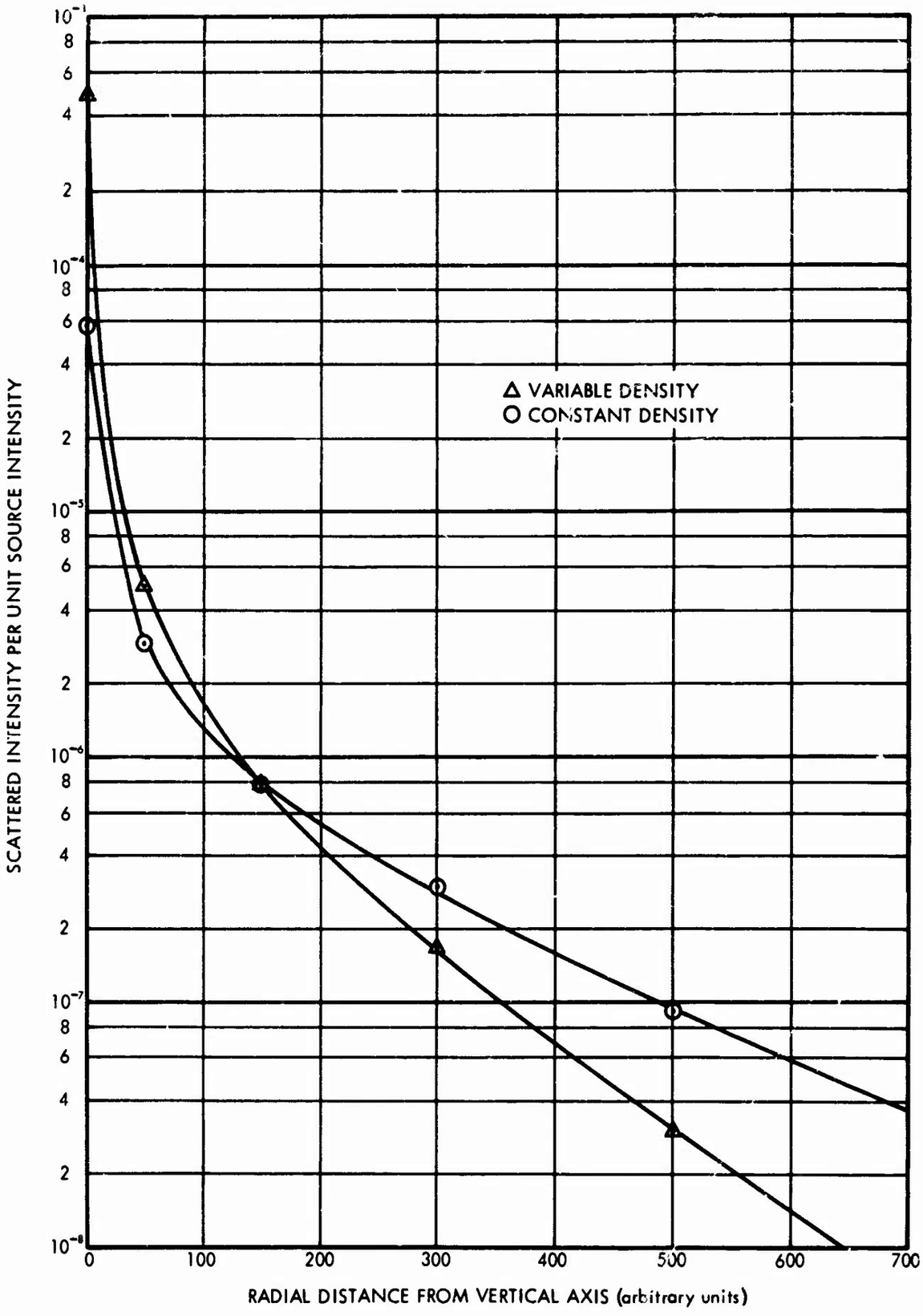

Fig. 12. Scattered Intensity Transmitted through a 0.5 Mean-Free-Path Thick Rayleigh Atmosphere: Normal Incident Line Beam Source, Albedo = 0.0

et al. (Reference 18) for one-velocity neutron diffusion problems. The first problem considered was for a plane isotropic source embedded within an infinite medium in which scattering was isotropic in the laboratory system, and the scattering-to-total cross section ratio was 0.5. Beach reported calculations of the total intensity as a function of distance from the plane source. The LITE-I code was run to give the intensity at point receivers located at several distances from a point isotropic source. The intensity was then multiplied by $4\pi R^2$ and plotted as a function of the distance R from the point source as shown in Figure 13. It is thought that the point at 900 units is probably an underprediction of the intensity, since sampling at this distance from the source would be inadequate unless some biasing scheme is used. Therefore, the curve, as drawn through the previous four points, was extrapolated to predict the intensity at 900 units and larger distances.

To apply the LITE-I code results to obtain the intensity at a distance h below a plane isotropic source, the following integral was evaluated

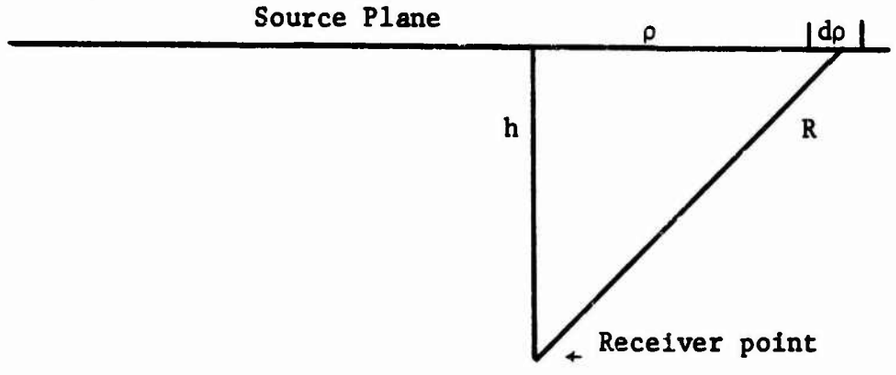

$$I(h) = \int_0^\infty \frac{2\pi I_o G(R)\rho\, d\rho}{4\pi R^2} \qquad 4.1.1$$

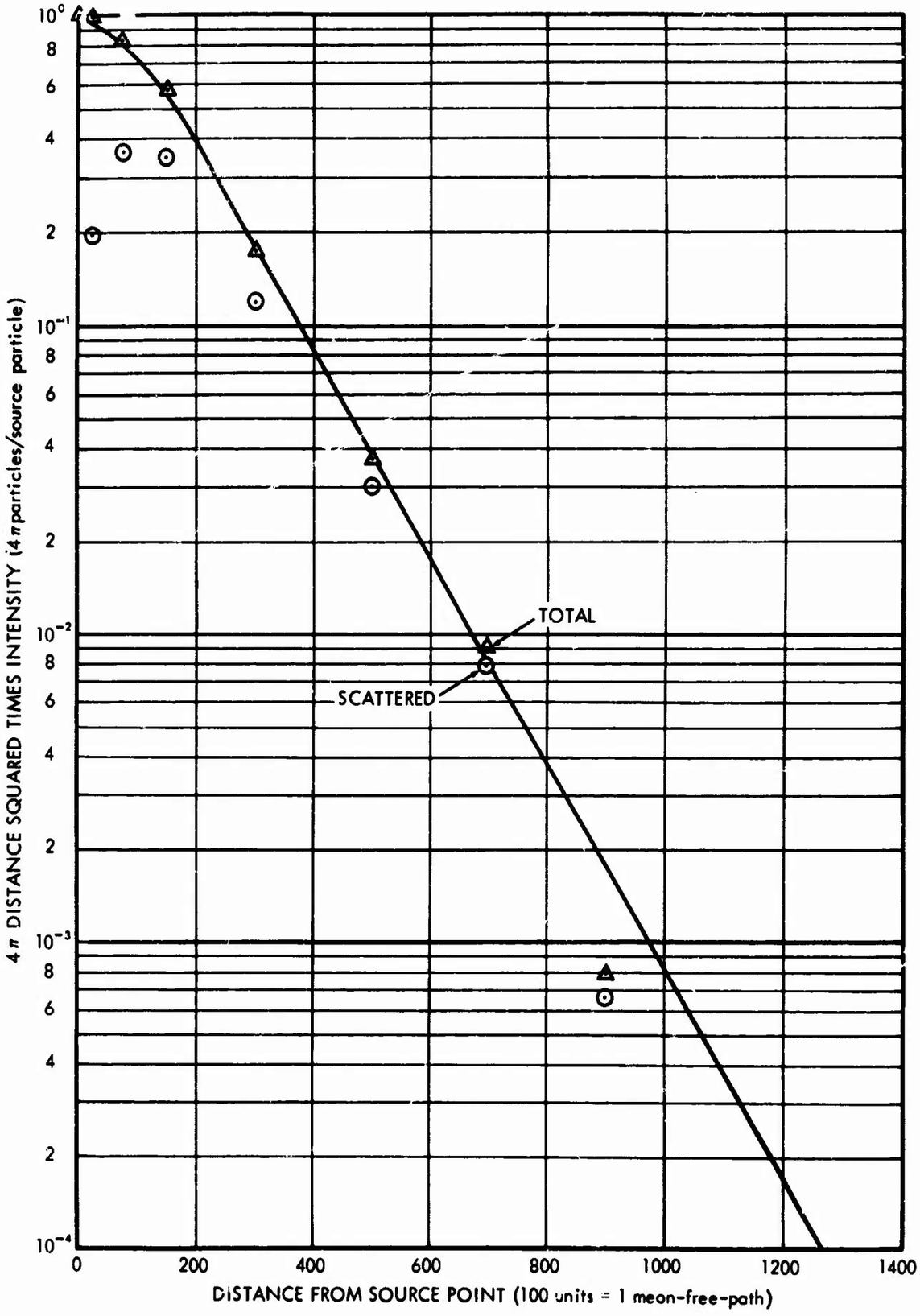

Fig. 13. $4\pi R^2$ Times Intensity as o Function of Distance from o Point Isotrapic Saurce in on Infinite Medium: Scattering-to-Tatol Cross Section Ratio = 0.5

where G(R) is $4\pi R^2$ times the intensity at distance R from a point isotropic source. By making the substitutions

$$\rho = h \tan\theta$$

$$d\rho = h \sec^2\theta d\theta$$

$$R = h \sec\theta$$

equation 4.1.1 becomes

$$I(h) = \frac{I_o}{2} \int_0^{\pi/2} G(R = h\sec\theta)\tan\theta d\theta \qquad 4.1.2$$

Equation 4.1.2 was integrated numerically for values of h corresponding to optical distances of τ = 1.1, 2.2, 4.1, 5.5 and 8.3. A comparison between Beach's data and the integrated LITE-I code results is shown in Figure 14.

A second comparison was made between LITE code results and Beach's data for a plane parallel source embedded within an infinite media in which all scattering was taken to be isotropic, and the scattering-to-total cross section ratio was 0.5. The LITE-I code was used to calculate the scattered intensity at points on three planes located 1, 2 and 3 optical distances below a point monodirectional source directed normal to the receiver planes. An integration of the intensities over the points in each plane was performed to obtain the total scattered intensity received by each plane. These integrated intensities were related to the intensity from a plane monodirectional source through the use of the reciprocity principle. A comparison of the scattered intensities derived from the LITE code results and those computed by Beach is shown in Figure 15.

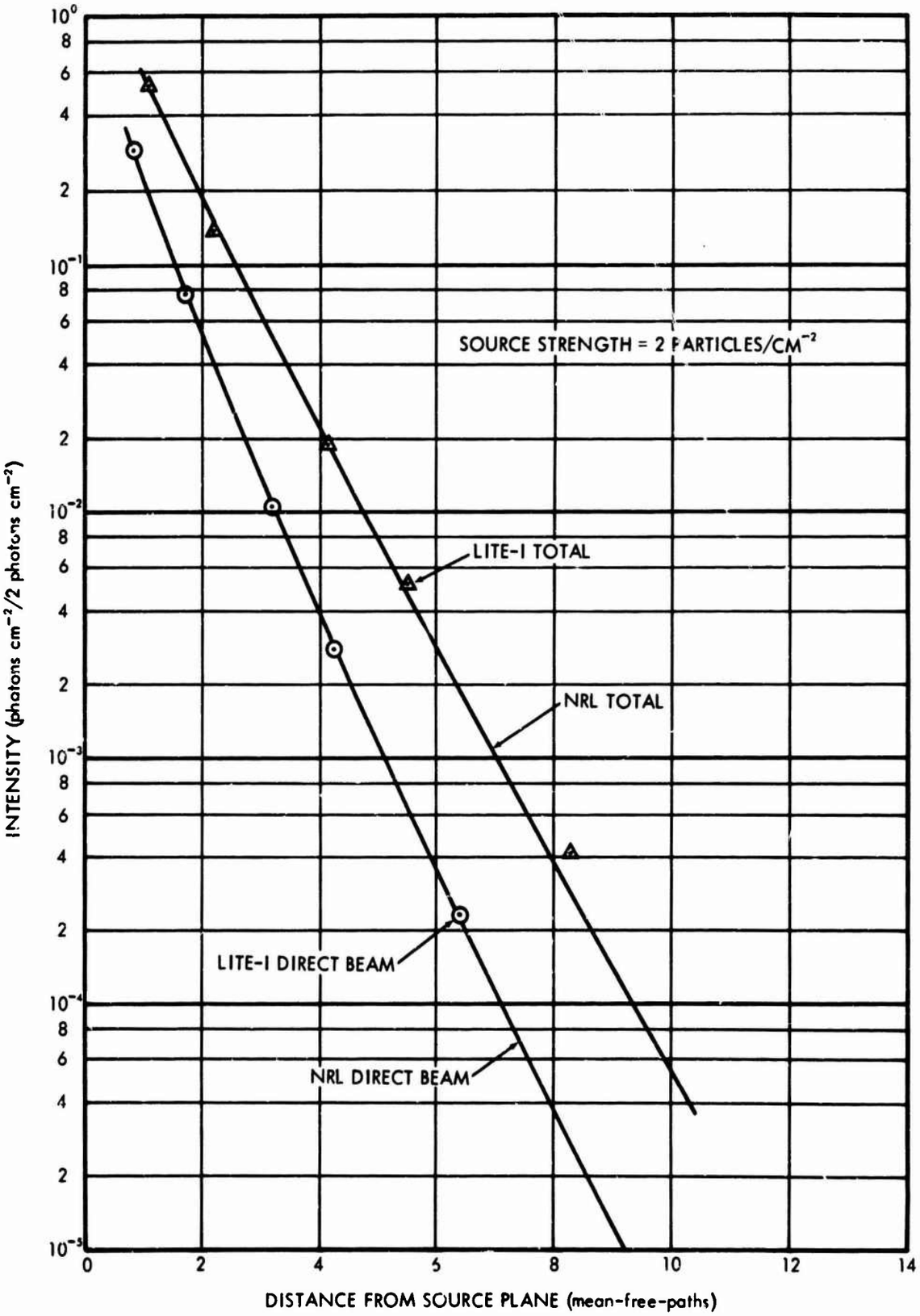

Fig. 14. Intensity Versus Distance from a Plane Isatropic Saurce in an Infinite Medium: Scattering-ta-Tatal Cross Sectian Ratio = 0.5

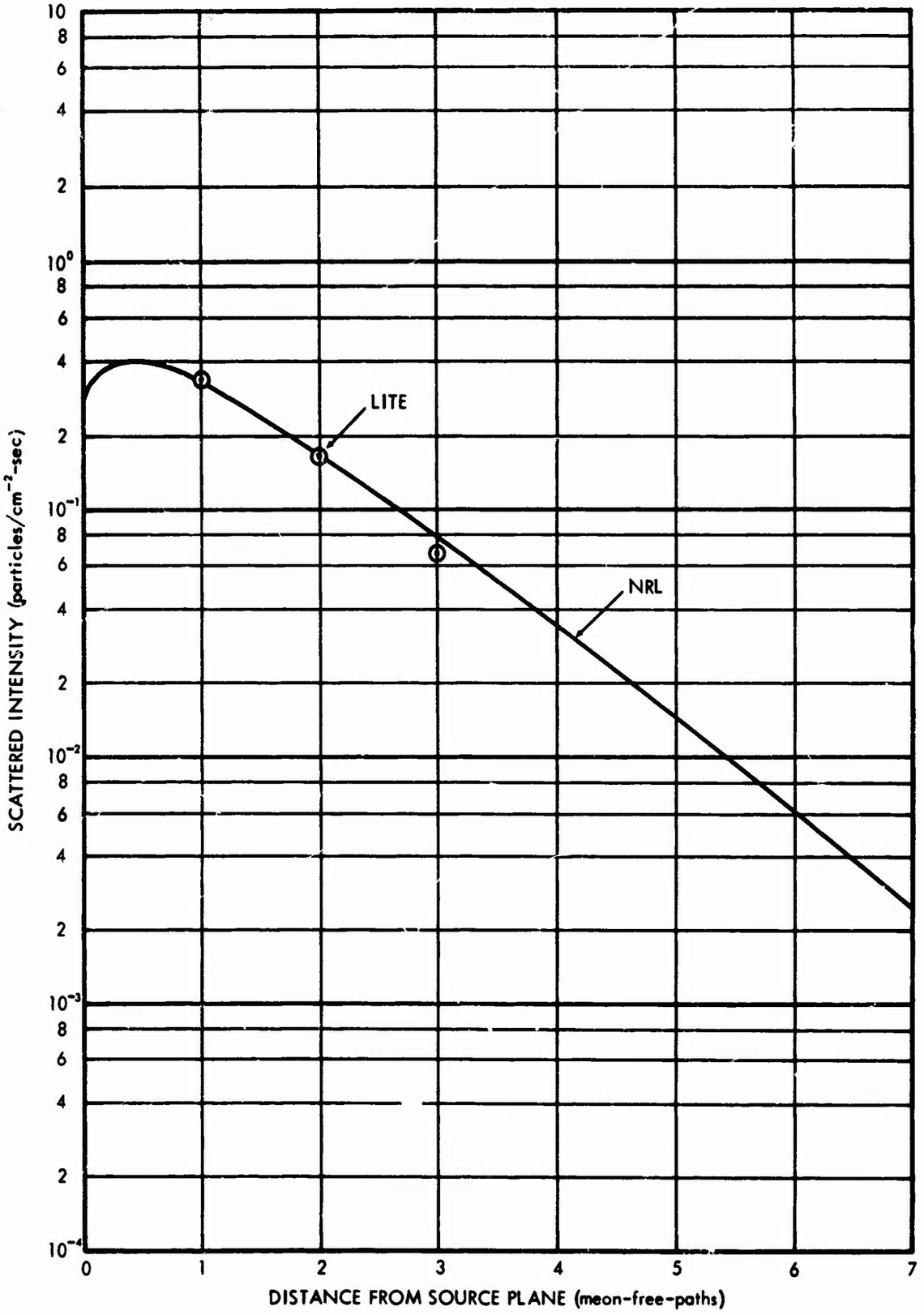

Fig. 15. Scattered Intensity as a Function of Distance from a Plane Parallel Monodirectional Source in an Infinite Medium: $\theta_0 = 0^\circ$, Scattering-to-Total Cross Section Ratio = 0.5

The good comparison between Beach's data and the LITE-I code indicates that the routines for treating Mie scattering are operating properly, since the isotropic scattering distributions were described in the problem input as Mie scattering.

4.2 LITE-II Code Results

Two problems for a 0.5 mean-free-path thick Rayleigh atmosphere were run with the LITE-II code to obtain results to compare with Coulson's data. The first problem was the same as the variable density problem run with the LITE-I code for a normal incident plane source and a 0.8 ground albedo. The second problem was for a plane source incident upon a 0.5 mean-free-path thick variable density Raleigh atmosphere at an angle of $\theta_o = \cos^{-1}0.6$. The second problem was also run for a ground albedo of 0.8. The results of the LITE-II code gives directly the intensity for a plane source incident upon the atmosphere, so no integration of the output data was necessary. For the two LITE-II problems, one receiver was placed in the atmosphere just slightly above the ground surface to record the transmitted scattered intensity. A second receiver was located just slightly below the surface defining the upper limit of the atmosphere to record the intensity reflected back out of the top of the atmosphere. Although the two problems were run for a ground albedo of 0.8, the results were also converted to data for ground albedos of 0.0 and 0.25 for comparison with Coulson's data for those albedos. Tables III and IV show a comparison of the data from the LITE-II code problems with Coulson's data. The data tabulated in Tables III and IV give the scattered intensity transmitted

Table III. Scattered Radiation Emerging from Upper and Lower Surfaces of a 0.5 Mean-Free Path Thick Rayleigh Atmosphere Due to a Normal Incident Plane Source

Albedo	Upper Surface		Lower Surface	
	LITE Code	Coulson Data	LITE Code	Coulson Data
0.0	.4442	.4422	.3694	.4025
0.25	.7007	.7106	.532	.5672
0.80	1.458	1.486	.9944	1.0321

Table IV. Scattered Radiation Emerging from the Upper and Lower Surfaces of a 0.5 Mean-Free-Path Thick Rayleigh Atmosphere Due to Plane Source Incident at $\theta_o = \cos^{-1}0.6$.

Albedo	Upper Surface		Lower Surface	
	LITE Code	Coulson Data	LITE Code	Coulson Data
0.0	.43	.4344	.38	.3768
0.25	.57	.5900	.47	.4424
0.80	.98	1.0028	.73	.7132

through or reflected from the atmosphere due to a unit intensity incident upon the top of the atmosphere. Angular distributions of the LITE-II calculated scattered intensities emerging from the atmosphere were also compared with Coulson's data. Figures 16 through 27 present comparisons of the LITE-II code calculated angular distributions at the upper and lower surfaces of the atmosphere for each of the three ground albedos for the normal incident plane source and the source incident at $\theta_o = \cos^{-1}0.6$. Coulson's angular distributions are given for a source term of π photons per unit area normal to the direction of travel. The angular distribution data obtained from the LITE-II output, have been multiplied by the same source term to produce the comparisons shown in Figures 16 through 27. The curves represent the intensity per steradian emitted from the atmosphere as a function of the cosine of the angle measured from the surface normal.

Two C18 problems were run to provide data on the light intensity as a function of depth in a Rayleigh atmosphere for comparison with the results of a LITE-II code problem. The thickness of the atmosphere was taken to be 0.5 mean-free-paths. The ground albedo was taken to be zero and the source was taken to be incident normal to the top of the atmosphere. In the first C18 problem the atmospheric density was taken to be constant with altitude. In the second C18 problem, the slab atmosphere was divided into 5 subslabs whose thicknesses were defined by the equation

$$0.1 = \int_{h_{i-1}}^{h_i} 0.00625\, e^{-0.0125h}\, dh, \quad i = 1,5$$

$$h_{i-1} = 0 \text{ for } i = 1,$$

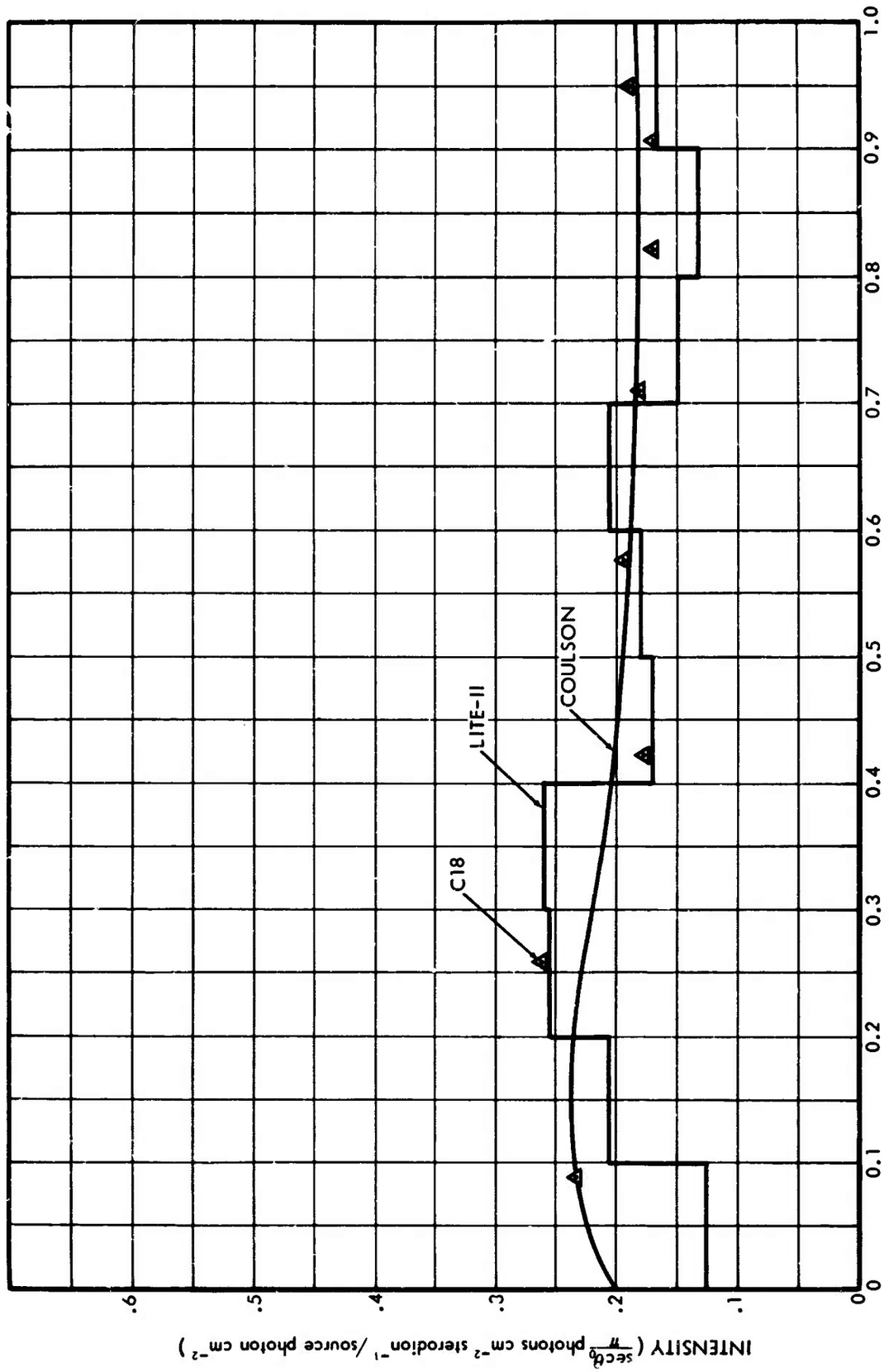

Fig. 16. Angular Distribution of the Scattered Radiation Transmitted through a 0.5 Mean-Free-Path Thick Rayleigh Atmosphere: $\theta_0=0^0$, Ground Albedo = 0.0

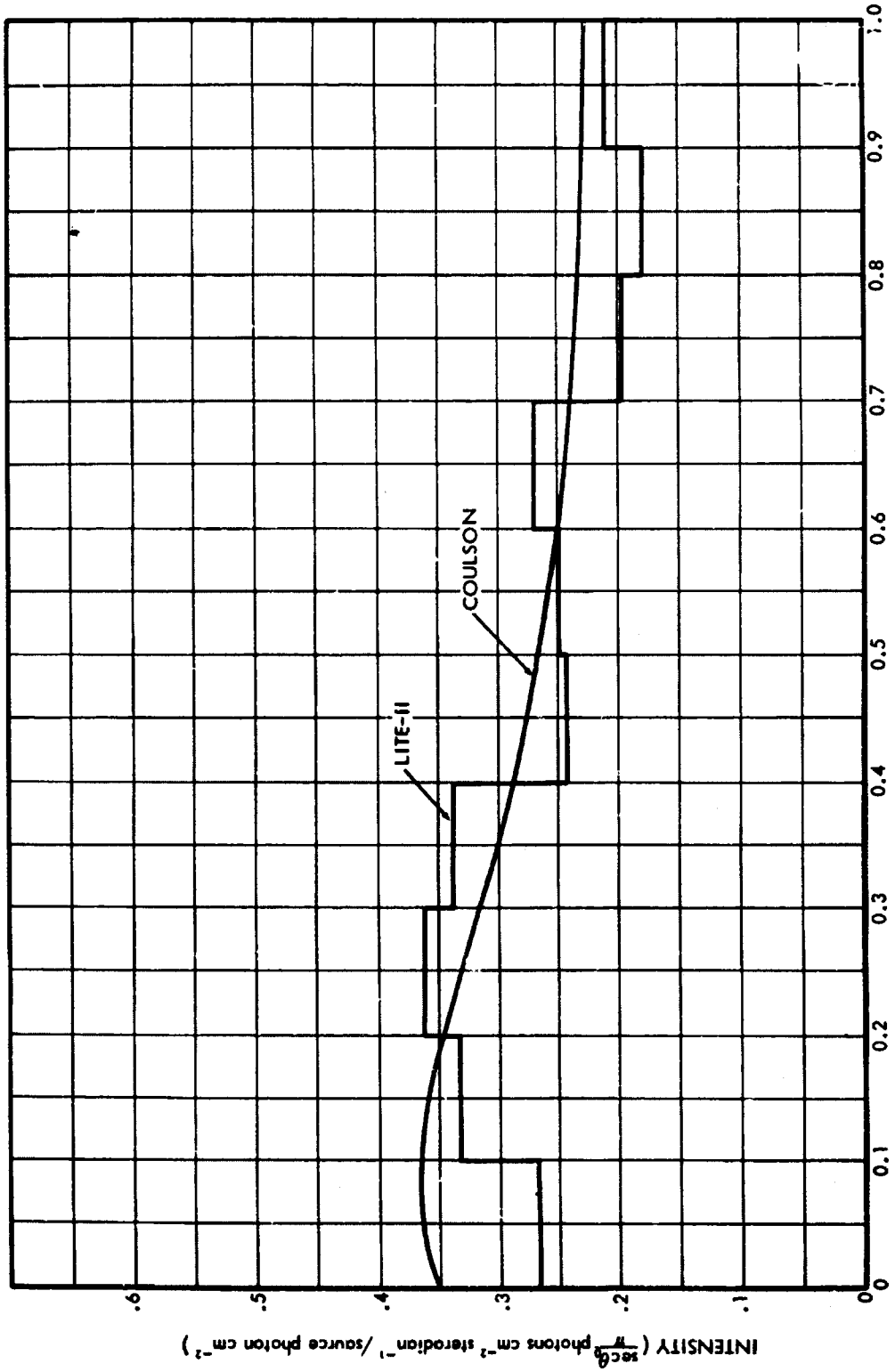

Fig. 17. Angular Distribution of the Scattered Radiation Transmitted through a 0.5 Mean-Free-Path Thick Rayleigh Atmosphere: $\theta_0 = 0°$, Ground Albedo = 0.25

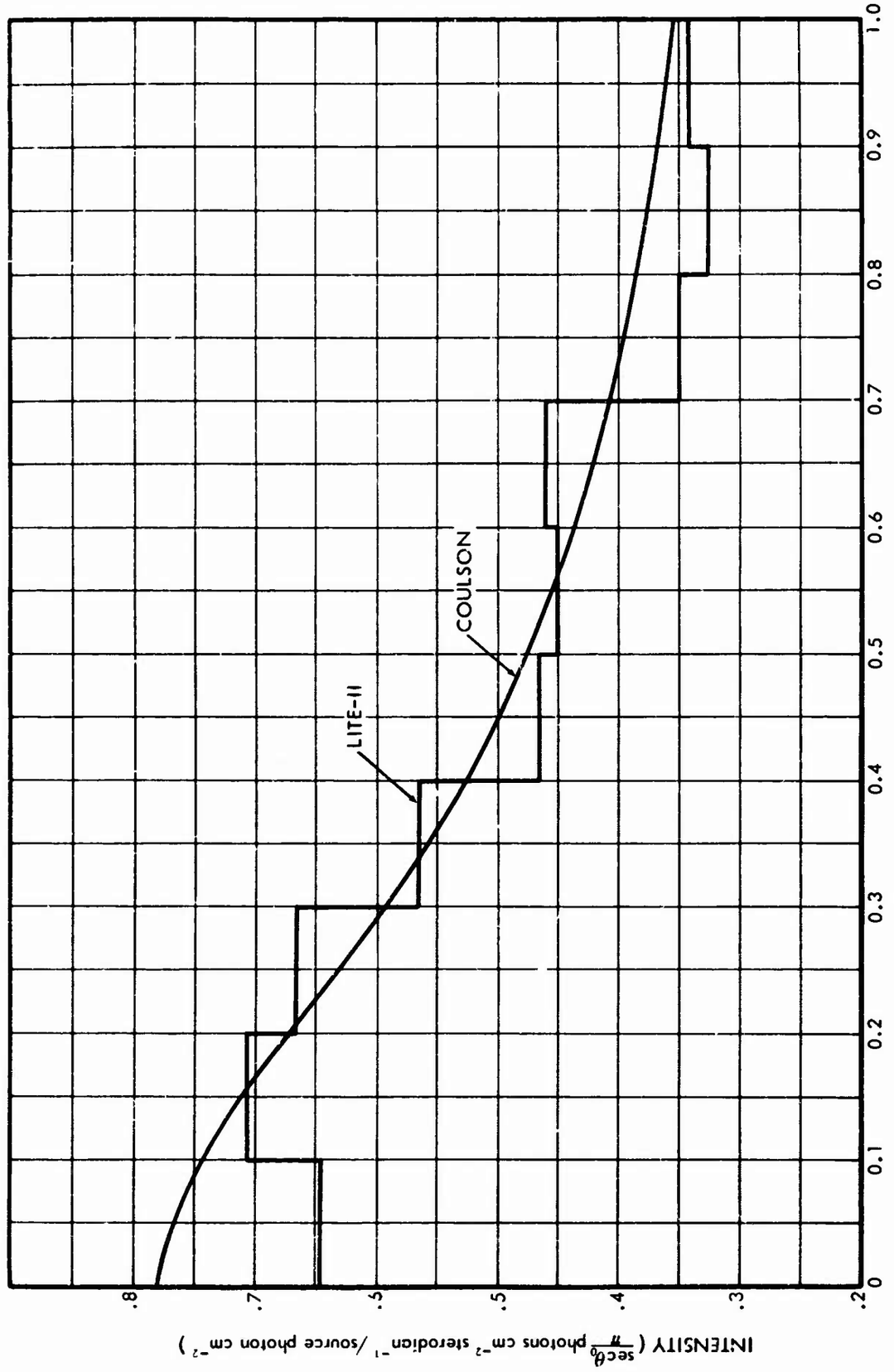

Fig. 18. Angular Distribution of the Scattered Radiation Transmitted through a 0.5 Mean-Free-Path Thick Rayleigh Atmosphere: $\theta_0 = 0^\circ$, Ground Albedo = 0.8

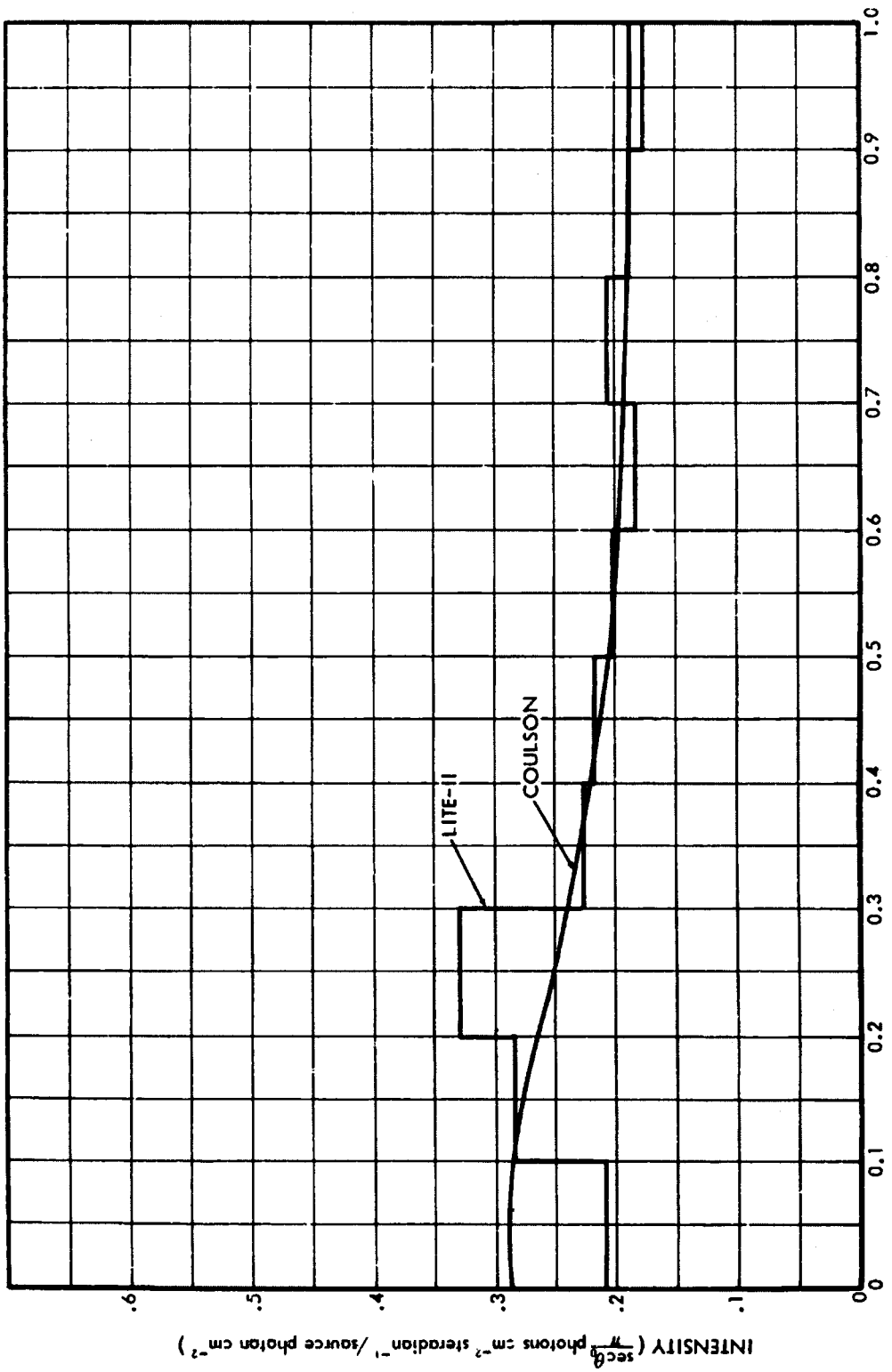

Fig. 19. Angular Distribution of the Radiation Reflected from a 0.5 Mean-Free-Path Thick Rayleigh Atmosphere: $\theta_0 = 0^0$ Ground Albedo = 0.0

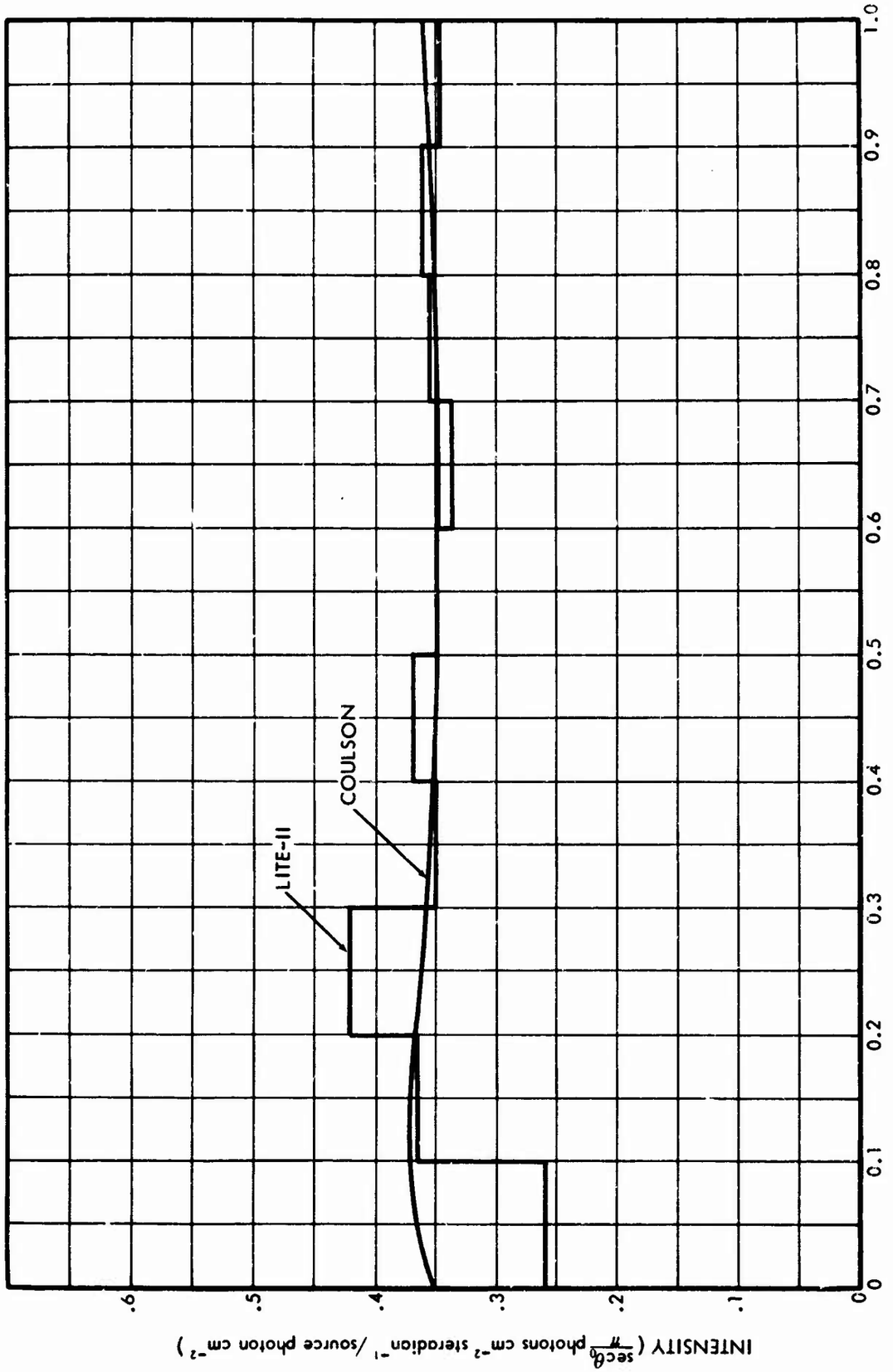

Fig. 20. Angular Distribution of the Radiation Reflected from a 0.5 Mean-Free-Path Thick Rayleigh Atmosphere: $\theta_0=0^o$, Ground Albedo = 0.25

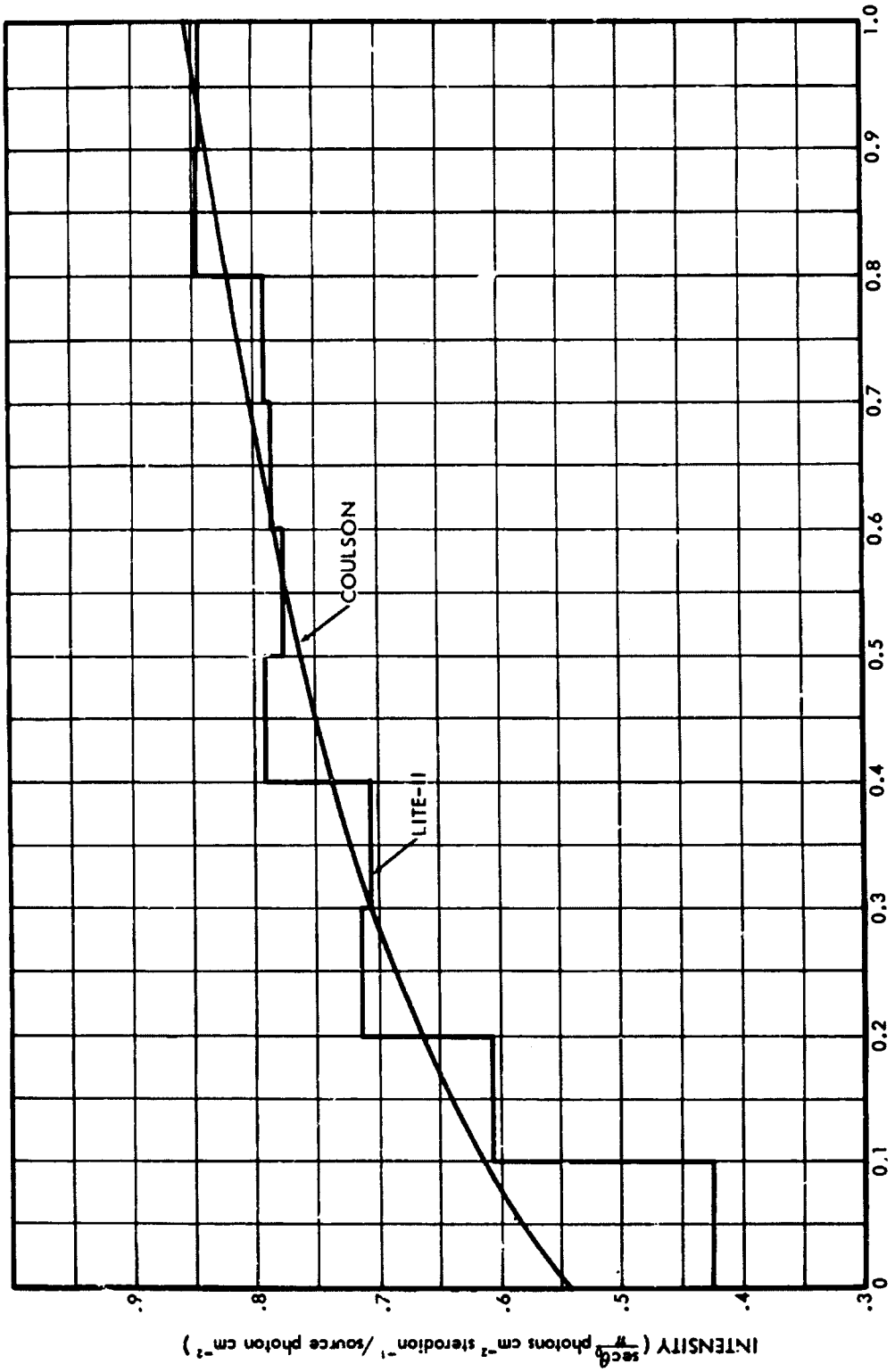

Fig. 21. Angular Distribution of the Radiation Reflected from a 0.5 Mean-Free-Path Thick Rayleigh Atmosphere: $\theta_0=0^\circ$, Ground Albedo = 0.8

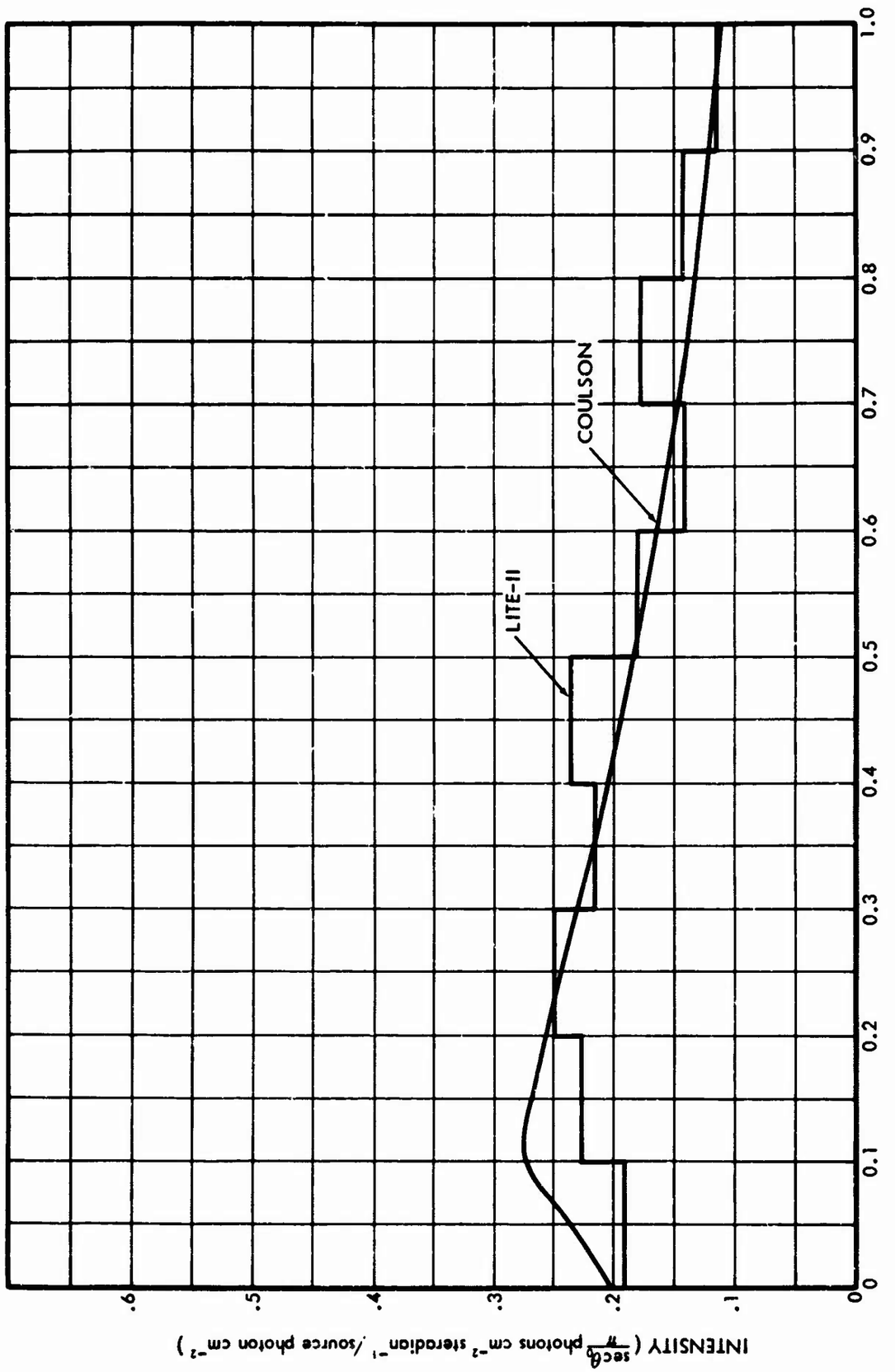

Fig. 22. Angular Distribution of the Scattered Radiation Transmitted through a 0.5 Mean-Free-Path Thick Rayleigh Atmosphere: $\theta_0 = \cos^{-1} 0.6$, Ground Albedo = 0.0

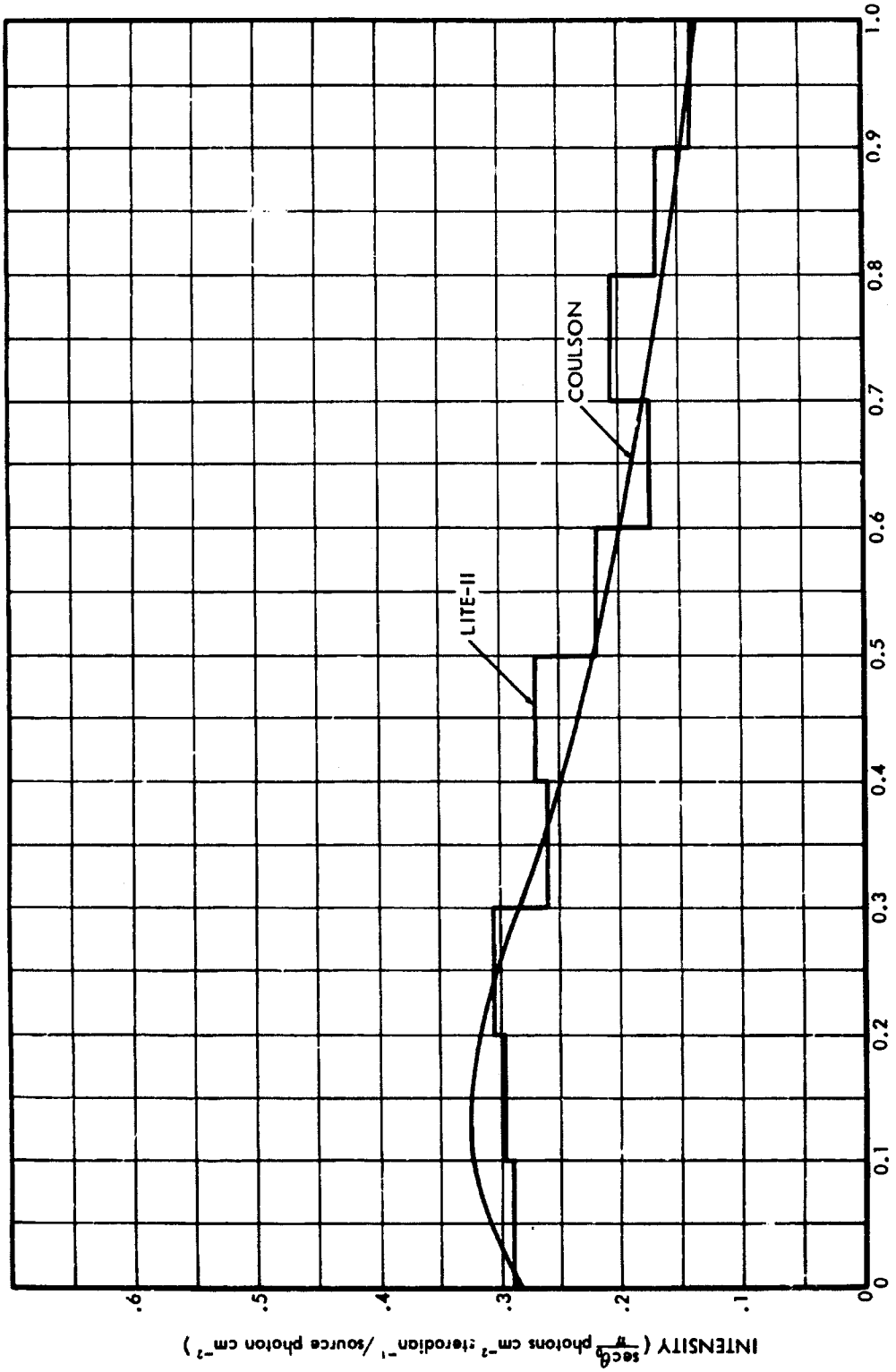

Fig. 23. Angular Distribution of the Scattered Radiation Transmitted through a 0.5 Mean-Free-Path Thick Rayleigh Atmosphere: $\theta_0 = \cos^{-1} 0.6$, Ground Albedo = 0.25

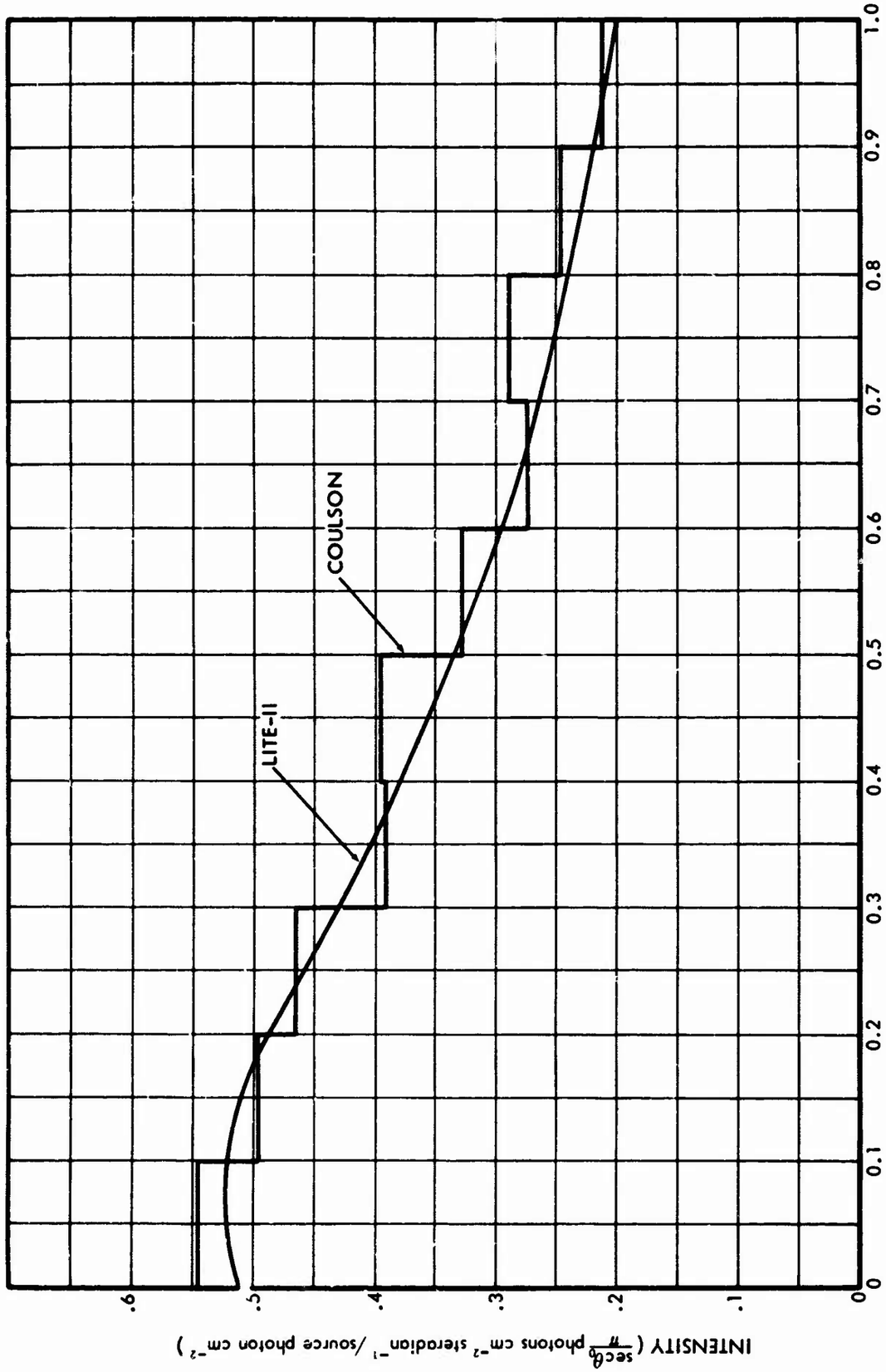

Fig. 24. Angular Distribution of the Scattered Radiation Transmitted through a 0.5 Mean-Free-Path Thick Rayleigh Atmosphere: $\theta_0 = \cos^{-1} 0.6$, Ground Albedo = 0.8

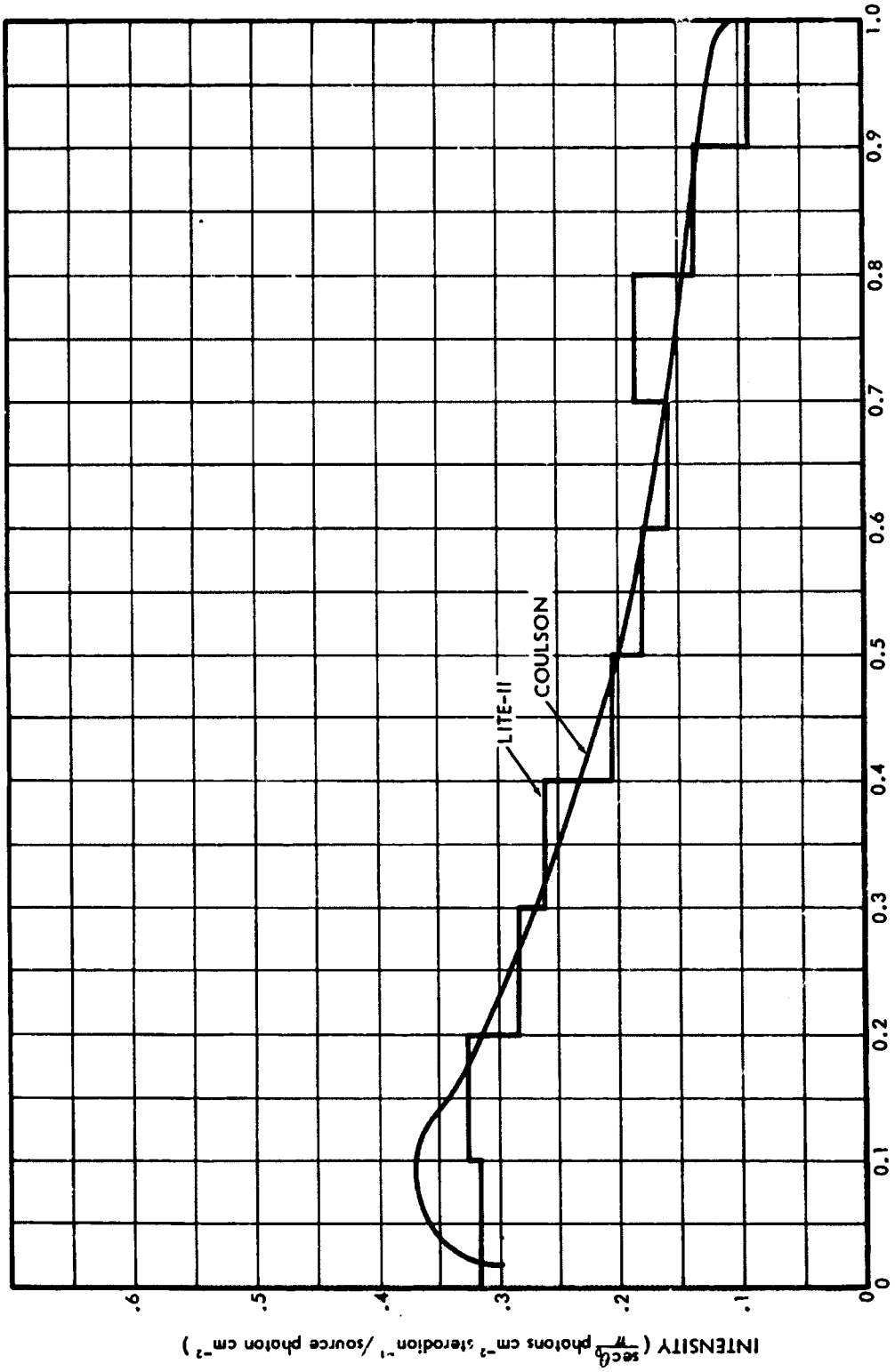

Fig. 25. Angular Distribution of the Radiation Reflected from a 0.5 Mean-Free-Path Thick Rayleigh Atmosphere: $\theta_0 = \cos^{-1} 0.6$, Ground Albedo = 0.0

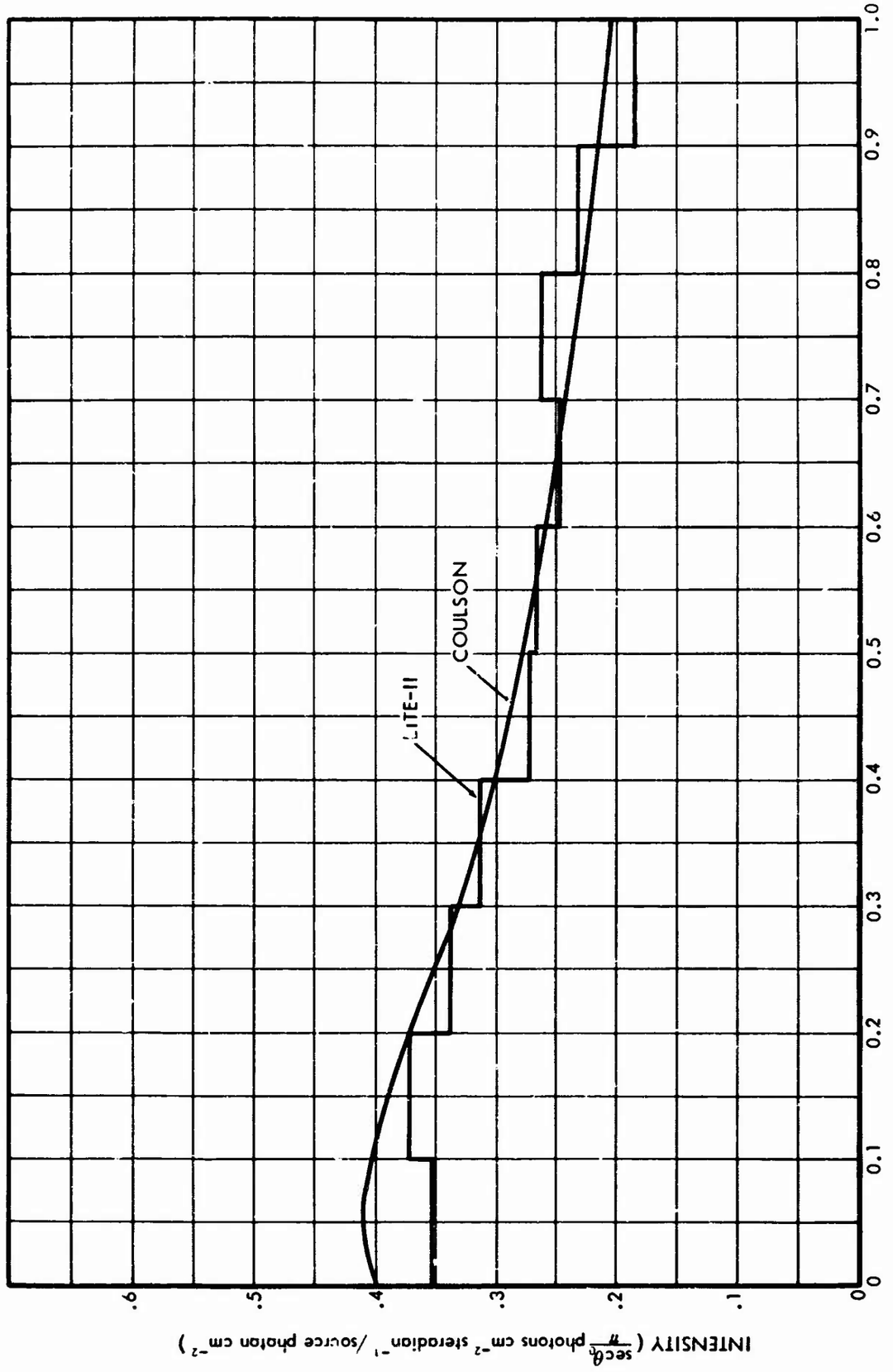

Fig. 26. Angular Distribution of the Radiation Reflected from a 0.5 Mean-Free-Path Thick Rayleigh Atmosphere: $\theta_0 = \cos^{-1}0.6$, Ground Albedo = 0.25

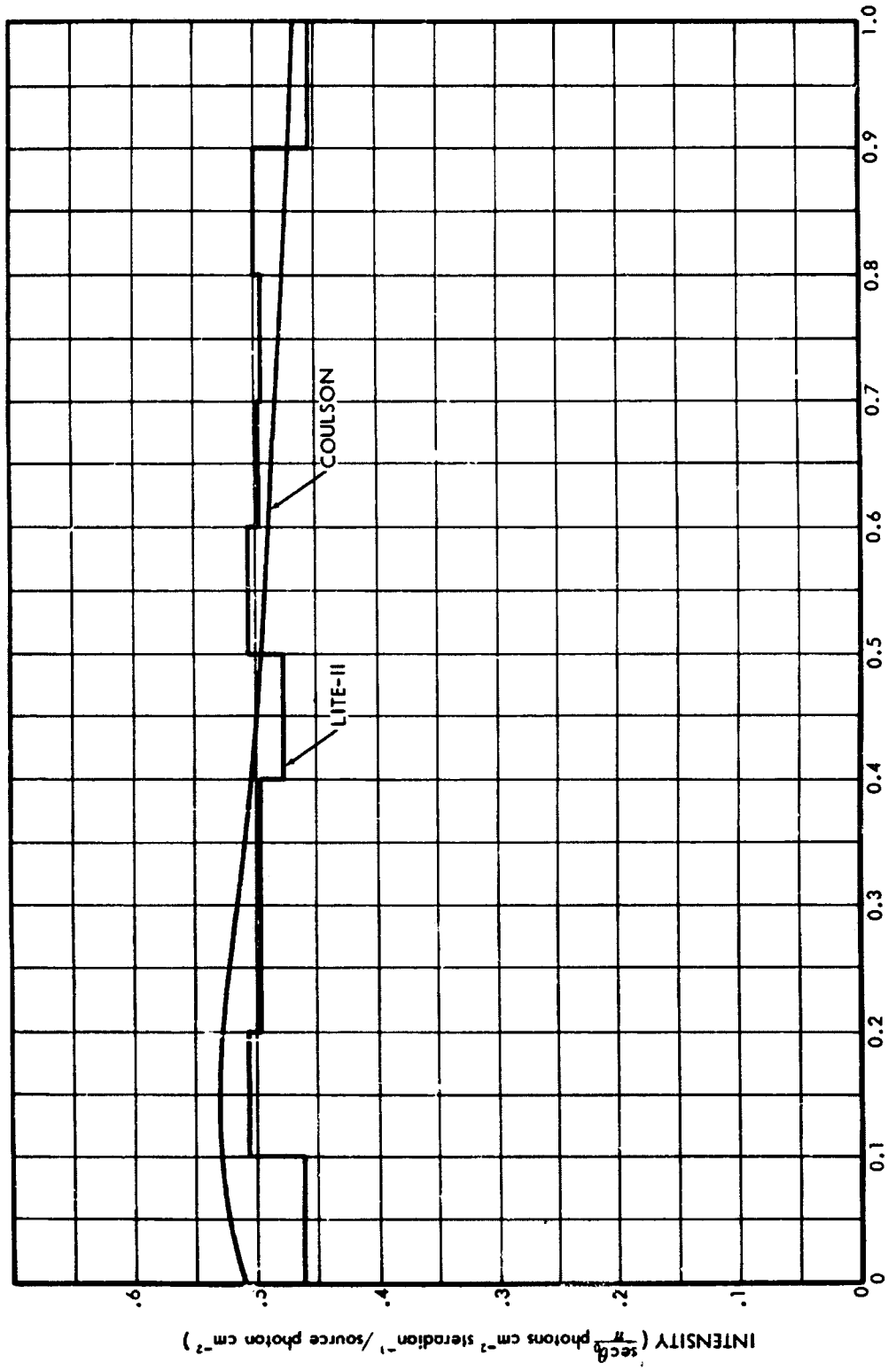

Fig. 27. Angular Distribution of the Radiation Reflected from a 0.5 Mean-Free-Path Thick Rayleigh Atmosphere: $\theta_0 = \cos^{-1}0.6$, Ground Albedo = 0.8

where h_{i-1} and h_i are the distances from the bottom of the atmosphere to the bottom and top of each of the five subslabs respectively.

The results from the two C18 problems are presented in Figure 28 as a function of the detector depth into the atmosphere in mean-free-paths. The results from a LITE-II code problem in which the atmospheric density was assumed to vary exponentially with altitude are also presented in Figure 28. It is seen that, within the statistical variation of the Monte Carlo results, there is no significant differences between the calculated spatial distributions of the total intensity as given by the two different codes. When the data in Figure 28 were plotted as a function of distance in units of h instead of in mean-free-paths, it was found that the intensity at a given distance is dependent on the atmospheric density distribution assumed for each problem. The results of these comparisons also show that the emergent radiation intensity at the top and bottom of the atmosphere is independent of the atmospheric density distribution assumed for each problem.

The angular distribution of the scattered intensity emerging from the bottom of a 0.5 mean-free-path thick Rayleigh atmosphere as given by the C18 calculations for a variable air density, are presented in Figure 16, where they can be compared with similar results obtained from the LITE-II code and from Coulson's data. It is seen that results from the three different calculations are in reasonably good agreement considering the small sample sizes used in the LITE-II and C18 Monte Carlo calculations.

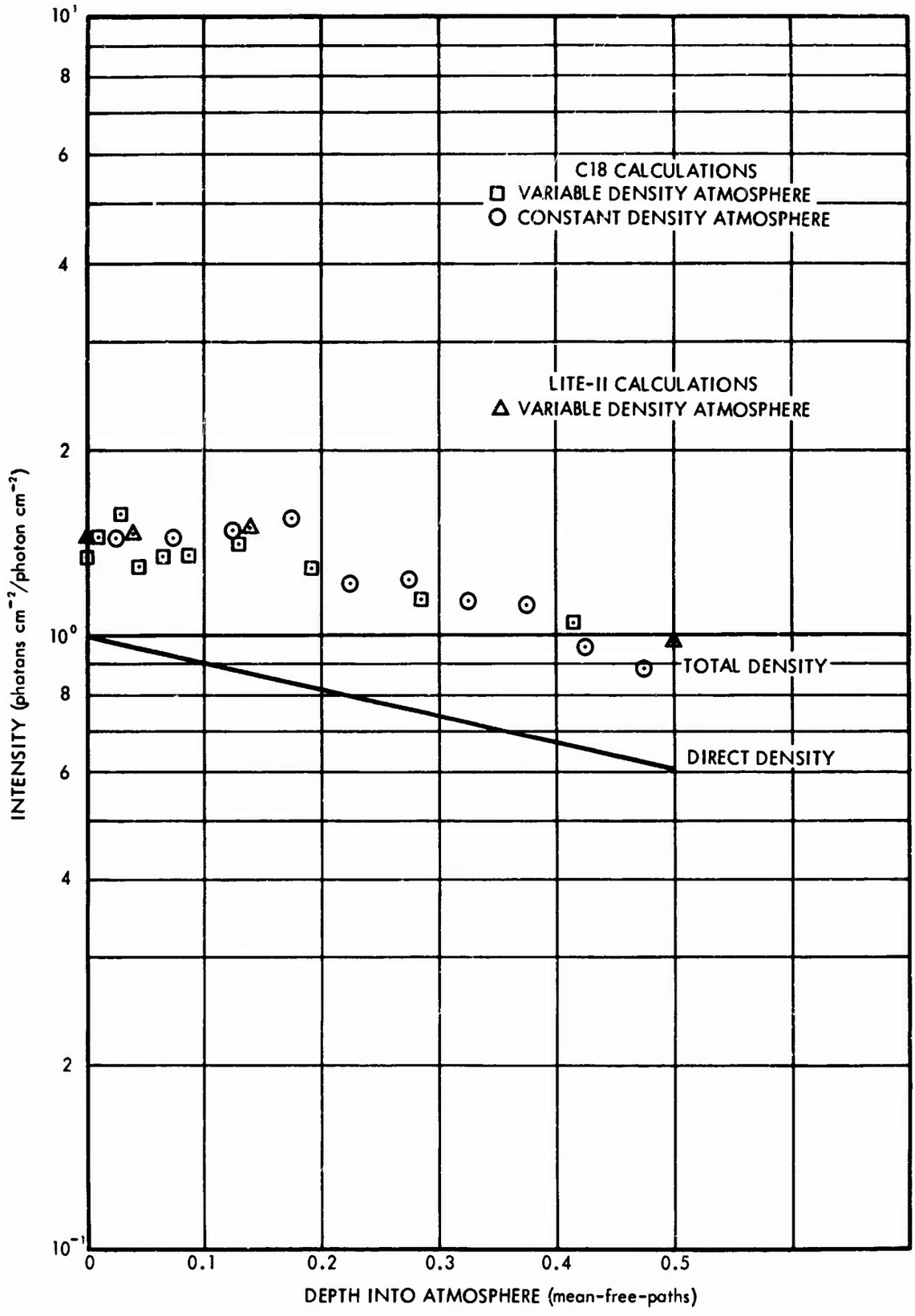

Fig. 28. Spatial Distributian af the Radiatian Intensity as a Functian af Depth inta a 0.5 Mean-Free-Path Thick Rayleigh Atmasphere: Narmal Incident Plane Parallel Saurce

REFERENCES

1. Cantor, I. and Petriw, A., Atmospheric Attenuation of Light Radiation from a Point Source in an Arctic Environment, United States Army Electronics Command Technical Report ECOM-2453, October 1964.

2. Curcio, J. A. and Drummeter, L. F., Jr., Experimental Observations of Forward Scattering of Light in the Lower Atmosphere, United States Naval Research Laboratory Report 6152, 30 September 1964.

3. Stewart, H. S. and Curcio, J. A., "The Influence of Field of View on Measurements of Atmospheric Transmission", J. Opt. Soc. Am., 42, 801 (1952).

4. Curcio, J. A., Knestrick, G. L. and Cosden, T. H., The Transmission of Light Signals Beyond the Horizon, NRL Report 5676, October 1961.

5. Curcio, J. A., Knestrick, G. L. and Cosden, T. H., Atmospheric Scattering in the Visible and Infrared, NRL Report 5567, January 1961.

6. Gibbons, M. G., et al., Transmission and Scattering Properties of a Nevada Desert Atmosphere, U. S. Naval Radiological Defense Laboratory Technical Report, USNRDL-TR-439, 12 November 1959.

7. Gibbons, M. G., et al., Transmission and Scattering Properties of a Nevada Atmosphere Under Cloudy Conditions, United States Naval Radiological Defense Laboratory Technical Report, USNRDL-TR-461, August 1960.

8. Gibbons, M. G., "Experimental Study of the Effect of Field of View on Transmission Measurements", J. Opt. Soc. Am., 49, 702 (1959).

9. Schleiger, E. R., Nichols, J. R. and Laughridge, F. I., Transmission and Scattering Properties of the Los Angeles, California Atmosphere in August and September 1960, U. S. Naval Radiological Defense Laboratory Technical Report, USNRDL-TR-554, October 1961.

10. Coulson, K. L., Dave, J. V., and Sekera, Z., Tables Related to Radiation Emerging from a Planetary Atmosphere with Rayleigh Scattering, University of Calfornia Press, Berkeley and Los Angeles, 1960.

11. Chandrasekhar, S., Radiative Transfer, Dover Publications, Inc., New York, New York, 1960.

12. Stewart, H. S., and Curcio, J. A., J. Opt. Soc. Am. 48, 550, 1958.

13. Collins, D. G., Utilization Instructions for General Application of the L05 Monte Carlo Procedure, Radiation Research Associates Report RRA-T44, 29 May 1964.

14. Rafalski, Pawel, "Evaluation of Albedo of Neutrons for Slab Wall", Nuclear Science and Engineering 19, No. 3, July 1964.

15. Wells, M. B., Monte Carlo Calculations of Fast-Neutron Energy Spectra, Convair-Fort Worth Report FZM-1267, December 1958, (Paper presented at the Sixth ANP Shielding Information Meeting, 2-3 December 1958).

16. Wells, M. B., Radiation Resistant Combat Vehicle Investigation-Final Report Volume III: Monte Carlo Multilayer Slab Geometry Shielding Code C-18, General Dynamics/Fort Worth Report FZK-134-3, December 1961.

17. Elterman, L., Atmospheric Attenuation Model, 1964, in the Ultraviolet, Visible and Infrared Regions for Altitudes to 50 km, Air Force Cambridge Research Laboratories Report AFLRL-64-740, September 1964.

18. Beach, L. A. et al., Comparison of Solutions to the One-Velocity Neutron Diffusion Problem, Naval Research Laboratory Report 5052, 23 December 1957.

DISTRIBUTION LIST

ADDRESSEE	NO. COPIES
Defense Documentation Center, ATTN: TISIA, Cameron Station (Bldg. 5) Alexandria, Virginia 22314	20
Commanding General, U. S. Army Materiel Command, ATTN: R&D Directorate, Washington, D. C. 20310	2
Chief, Research and Development, Department of the Army, ATTN: CRD M, Washington, D. C. 20315	2
Director, DASA, ATTN: DASARA-5, Washington, D. C. 20315	4
Commanding General, U. S. Army Electronics Command, ATTN: AMSEL-IO-T, Fort Monmouth, New Jersey 07703	1
Commanding General, U. S. Army Electronics Command, ATTN: AMSEL-EW, Fort Monmouth, New Jersey 07703	2
Commanding General, U. S. Army Electronics Command, ATTN: AMSEL-RD-ADT, Fort Monmouth, New Jersey 07703	1
Commanding General, U. S. Army Electronics Command, ATTN: AMSEL-RD-ADO-RHA, Fort Monmouth, New Jersey 07703	1
Commanding General, U. S. Army Electronics Command, ATTN: AMSEL-BL-D, Fort Monmouth, New Jersey 07703	2
Commanding General, U. S. Army Electronics Command, ATTN: AMSEL-BL-MA, Fort Monmouth, New Jersey 07703	15
Director, U. S. Naval Research Laboratory, ATTN: Code 2027 Washington, D. C. 20390	2
Commander, Air Force Cambridge Research Laboratories, ATTN: CRXL-R, L. G. Hanscom Field, Bedford, Massahcusetts 01731	2
Commander, Air Force Cambridge Research Laboratories, ATTN: CROA, L. G. Hanscom Field, Bedford, Massachusetts 01731	4
Air Weather Service (MATS), U. S. Air Force, ATTN: AWSAE Scott Air Fource Base, Illinois	2
Commanding Officer, U. S. Army Electronics R&D Activity, ATTN: SELHU-PT, Fort Huachuca, Arizona 85613	2
Commanding General, U. S. Army Electronic Proving Ground ATTN: Technical Library, Fort Huachuca, Arizona 85613	1

ADDRESSEE	NO. COPIES
Commanding Officer, U. S. Army Electronics R&D Activity, ATTN: SELWS-MT, White Sands Missile Range, New Mexico	2
Institute of Science and Technology, The University of Michigan, P. O. Box 613, ATTN: Background Library, Ann Arbor, Michigan 48107	1
NASA Representative, Scientific and Technical Information Facility, P. O. Box 5700, Bethesda, Maryland 20014	2
Redstone Scientific Information Center, Redstone Arsenal, Alabama	2
The American Meteorological Society, Abstracts & Bibliography P. O. Box 1736, ATTN: Mr. M. Rigby, Washington, D. C.	2
Library, U. S. Weather Bureau, Washington, D. C.	2
Director, Atmospheric Sciences Programs, National Science Foundation, Washington, D. C.	2
Commanding General, Army Ordnance Missile Command, ATTN: ORDXM/RRA, Dr. O. M. Essenwanger, Redstone Arsenal, Alabama	2
Commanding Officer, U. S. Army Electronics R&D Activity, ATTN: Missile Geophysics Division, White Sands Missile Range, New Mexico	2
Office of Technical Services, Department of Commerce, Washington, D. C.	2
Director, Atmospheric Science and Chemical Laboratory, ESSA, U. S. Weather Bureau, Washington, D. C.	2
University of Chicago, ATTN: Rosenwald Library, Department of the Geophysical Sciences, 1101 E. 58th Street, Chicago, Illinois 60637	2
New York University, College of Engineering, University Heights, New York 53, New York	2
DASA Data Center, 735 State Street, Santa Barbara, California 93102	2
Meteorology Department, Pennsylvania State College, State College, Pennsylvania	1
Department of Meteorology, Massachusetts Institute of Technology, Cambridge, 39, Massachusetts	2
U. S. Army Natick Laboratories, ATTN: Earth Sciences Division, Natick, Massachusetts	2

ADDRESSEE	NO. COPIES
U. S. National Bureau of Standards, Boulder Laboratories ATTN: Library, Boulder, Colorado	1
National Center Atmospheric Sciences, Boulder, Colorado	1
University of Miami, ATTN: Radar Met. Laboratory, Mr. Homer Hiser P. O. Box 8003, Coral Gables, Florida 33124	2
Intermountain Weather Incorporated, P. O. Box 88, Salt Lake City, Utah	1

Unclassified

Security Classification

DOCUMENT CONTROL DATA - R&D

(Security classification of title, body of abstract and indexing annotation must be entered when the overall report is classified)

1. ORIGINATING ACTIVITY *(Corporate author)*
RADIATION RESEARCH ASSOCIATES, INC.
Fort Worth, Texas

2a. REPORT SECURITY CLASSIFICATION
Unclassified

2b GROUP

3. REPORT TITLE
MONTE CARLO CODES FOR STUDY OF LIGHT TRANSPORT IN THE ATMOSPHERE, VOLUME I: DESCRIPTION OF CODES

4. DESCRIPTIVE NOTES *(Type of report and inclusive dates)*
Final Report 1 July 1964 to 31 July 1965

5. AUTHOR(S) *(Last name, first name, initial)*
Collins, David G. and Wells, Michael B.

6. REPORT DATE	7a. TOTAL NO. OF PAGES	7b. NO. OF REFS
August 1965	90	18

8a. CONTRACT OR GRANT NO.
DA 28-043 AMC-00240(E)

b. PROJECT NO.
DA TASK NO. 5900-21-830-55

c.

d.

9a. ORIGINATOR'S REPORT NUMBER(S)
RRA-T54-1

9b. OTHER REPORT NO(S) *(Any other numbers that may be assigned this report)*
ECOM-00240-F, Vol. I

10. AVAILABILITY/LIMITATION NOTICES
Qualified requesters may obtain copies of this report from DDC.
This report has been released to CFSTI.

11. SUPPLEMENTARY NOTES

12. SPONSORING MILITARY ACTIVITY
U. S. Army Electronics Command
Fort Monmouth, New Jersey

13. ABSTRACT

Monte Carlo procedures designated as the LITE-I and LITE-II codes were developed to study the transport of light through the earth's atmosphere under various environmental conditions. The LITE-I code treats monochromatic light emitted from a point source, and the LITE-II code treats monochromatic plane sources of light. The codes have been written in both ALGOL for the Burroughs B-5000 and FORTRAN II for other computers. The codes are sufficiently flexible to treat multiple scattering in an atmosphere in which air density and aerosol size distribution vary independently and arbitrarily with altitude. Provision for treating ground and cloud reflection with an albedo method is also available in the codes.

The codes have been varified through comparisons with other calculations of light transport in the atmosphere. Utilization instructions, input data formats, sample problems, and the ALGOL listings of the codes are given to aid those who wish to utilize the codes.

DD FORM 1 JAN 64 1473

Unclassified

Security Classification

14. KEY WORDS	LINK A		LINK B		LINK C	
	ROLE	WT	ROLE	WT	ROLE	WT
Monte Carlo Methods Light transmission Radiation Transport Variable density atmosphere Albedo Point Source Plane Source Multiple Scattering Mie Scattering Rayleigh Scattering						

INSTRUCTIONS

1. ORIGINATING ACTIVITY: Enter the name and address of the contractor, subcontractor, grantee, Department of Defense activity or other organization *(corporate author)* issuing the report.

2a. REPORT SECURITY CLASSIFICATION: Enter the overall security classification of the report. Indicate whether "Restricted Data" is included. Marking is to be in accordance with appropriate security regulations.

2b. GROUP: Automatic downgrading is specified in DoD Directive 5200.10 and Armed Forces Industrial Manual. Enter the group number. Also, when applicable, show that optional markings have been used for Group 3 and Group 4 as authorized.

3. REPORT TITLE: Enter the complete report title in all capital letters. Titles in all cases should be unclassified. If a meaningful title cannot be selected without classification, show title classification in all capitals in parenthesis immediately following the title.

4. DESCRIPTIVE NOTES: If appropriate, enter the type of report, e.g., interim, progress, summary, annual, or final. Give the inclusive dates when a specific reporting period is covered.

5. AUTHOR(S): Enter the name(s) of author(s) as shown on or in the report. Enter last name, first name, middle initial. If military, show rank and branch of service. The name of the principal author is an absolute minimum requirement.

6. REPORT DATE: Enter the date of the report as day, month, year; or month, year. If more than one date appears on the report, use date of publication.

7a. TOTAL NUMBER OF PAGES: The total page count should follow normal pagination procedures, i.e., enter the number of pages containing information.

7b. NUMBER OF REFERENCES: Enter the total number of references cited in the report.

8a. CONTRACT OR GRANT NUMBER: If appropriate, enter the applicable number of the contract or grant under which the report was written.

8b, 8c, & 8d. PROJECT NUMBER: Enter the appropriate military department identification, such as project number, subproject number, system numbers, task number, etc.

9a. ORIGINATOR'S REPORT NUMBER(S): Enter the official report number by which the document will be identified and controlled by the originating activity. This number must be unique to this report.

9b. OTHER REPORT NUMBER(S): If the report has been assigned any other report numbers *(either by the originator or by the sponsor)*, also enter this number(s).

10. AVAILABILITY/LIMITATION NOTICES: Enter any limitations on further dissemination of the report, other than those imposed by security classification, using standard statements such as:

(1) "Qualified requesters may obtain copies of this report from DDC."

(2) "Foreign announcement and dissemination of this report by DDC is not authorized."

(3) "U. S. Government agencies may obtain copies of this report directly from DDC. Other qualified DDC users shall request through _____."

(4) "U. S. military agencies may obtain copies of this report directly from DDC. Other qualified users shall request through _____."

(5) "All distribution of this report is controlled. Qualified DDC users shall request through _____."

If the report has been furnished to the Office of Technical Services, Department of Commerce, for sale to the public, indicate this fact and enter the price, if known.

11. SUPPLEMENTARY NOTES: Use for additional explanatory notes.

12. SPONSORING MILITARY ACTIVITY: Enter the name of the departmental project office or laboratory sponsoring *(paying for)* the research and development. Include address.

13. ABSTRACT: Enter an abstract giving a brief and factual summary of the document indicative of the report, even though it may also appear elsewhere in the body of the technical report. If additional space is required, a continuation sheet shall be attached.

It is highly desirable that the abstract of classified reports be unclassified. Each paragraph of the abstract shall end with an indication of the military security classification of the information in the paragraph, represented as *(TS), (S), (C), or (U)*.

There is no limitation on the length of the abstract. However, the suggested length is from 150 to 225 words.

14. KEY WORDS: Key words are technically meaningful terms or short phrases that characterize a report and may be used as index entries for cataloging the report. Key words must be selected so that no security classification is required. Identifiers, such as equipment model designation, trade name, military project code name, geographic location, may be used as key words but will be followed by an indication of technical context. The assignment of links, rules, and weights is optional.